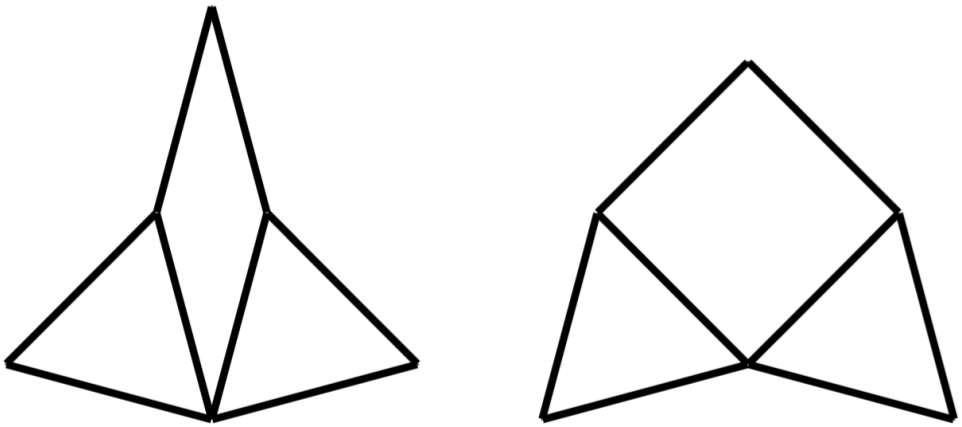

On the Number of Configurations of Triangular Mechanisms

THESIS

submitted in partial fulfillment of the
requirements for the degree of

BACHELOR OF SCIENCE
in
PHYSICS AND MATHEMATICS

Author :	R.M.A. Zandbergen
Student ID :	1260626
Supervisor Physics:	Prof. dr. Martin van Hecke
Supervisor Mathematics :	Dr. Floske Spieksma

Leiden, The Netherlands, July 21, 2016

On the Number of Configurations of Triangular Mechanisms

R.M.A. Zandbergen

Huygens-Kamerlingh Onnes Laboratory, Leiden University
P.O. Box 9500, 2300 RA Leiden, The Netherlands

Mathematical Institute Leiden, Leiden University
P.O. Box 9512, 2300 RA Leiden, The Netherlands

July 21, 2016

Abstract

In this thesis, we will give a way to build mechanical metamaterials. We will do this by using a triangular tiling, in which we put spins on the edges of the tiles. These spins have to point either into or out of the triangles and have to satisfy the rule that for every triangle two spins have to point out, and one in, or two spins point in and one out. If we can construct a tiling that is completely filled with these triangles in such a way that all spins on sides of adjacent triangles are pointing in the same direction, we will call this a feasible configuration. Firstly, we derive the number of feasible configurations for the tiling and consider a way to estimate these values. Secondly, we derive the distribution for the number of configurations when there are i spins on the boundary pointing in. Finally, we consider the number of spins in a periodic tiling that can be reversed, independent of all other spins, and derive an upper value and a lower boundary for this.

Contents

Chapter 1

Introduction

In this chapter an general overview of mechanical metamaterials will be given. We will introduce the triangular mechanisms we will be considering in this thesis. Definitions that might be relevant to remember throughout this thesis, can be found in Appendix B.

1.1 Mechanical metamaterials

As described in [1], mechanical metamaterials are media depending on their properties given by structure, rather than composition. These materials are designed by mankind, thus obtaining properties that have not been achieved by structures found in nature.

Nowadays, several of these mechanical metamaterials are known, and were made by using, among others, the 3D-printer. This offered the ability to create structures on the micro- and macro-scale. Examples of these mechanical metamaterials are media having properties like: being ultralightweight, as designed by Schaedler, et al. [2] (Figure 1.1a), being bistable [3] (Figure 1.1b) or having a negative Poisson's ratio [4] (Figure 1.1c) (the transversal length becomes smaller, when pressing along the axial direction).

Due to the 3D-printer, also pentamode materials, as proposed by Milton and Cherkaev [5] (Figure 1.1d) can be made, which are materials with a finite bulk modulus (resistance to uniform compression), but a vanishing shear modulus (resistance to shearing forces) [6]. These materials are hard to compress, but easy to deform. They ideally behave like a fluid, and can be used to make mechanical unfeelability cloaks [7].

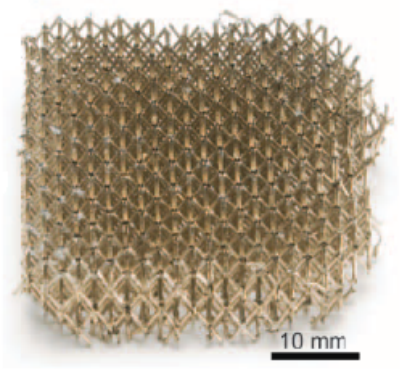

(a) *Ultralight microlattice, density of 0.9 mg/cm^3 [2].*

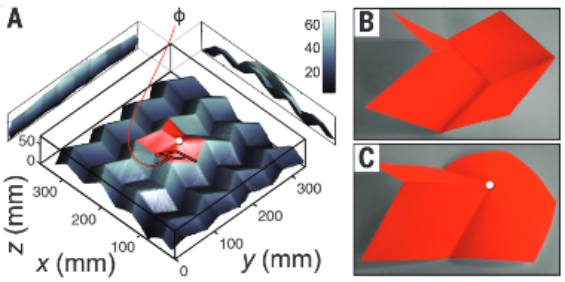

(b) ***A****: Reconstruction of a Miura folding, where the red faces have a pop-through defect, one of the folds is suppressed, while adjacent faces are bended.* ***B,C****: Photograph of single vertex (B) and it's pop-through defect (C), which are both stable. Edited from [3].*

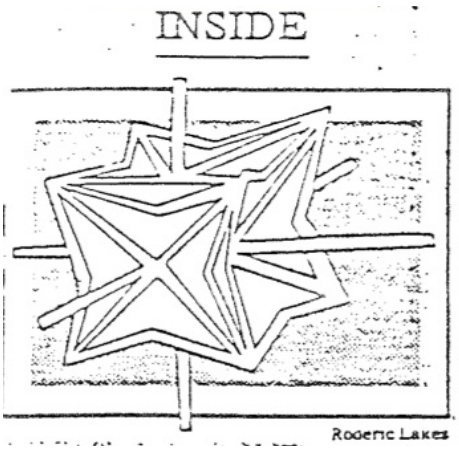

(c) *A unit cell of a material with a negative Poisson's ratio. Edited from [8].*

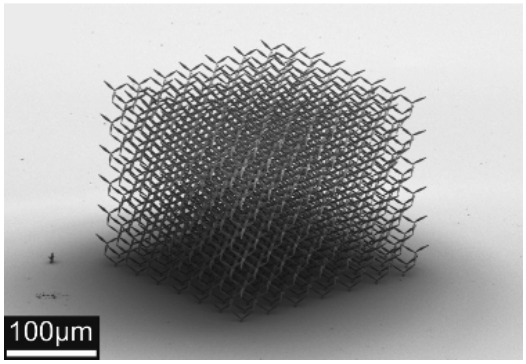

(d) *Electron micrograph of polymer pentamode material [6].*

Figure 1.1: *Mechanical Metamaterials*

In his thesis [9], Kettenis discusses the design of 2D mechanical metamaterials with simple unit cells. The Poisson's ratio (the negative ratio of the strain in the transversal direction over the strain in the axial direction, i.e. in the direction in which the load is applied) of these unit cells could in advance be programmed to be either negative or positive [9]. In Kettenis' thesis, a few of the possible different structures that can be made with these designs, are discussed.

Amongst these discussed structures are the following: one with a negative Poisson's ratio (so when they are expanded in one direction, they also expand in the other direction) as shown in Figure 1.2a, and one with a positive Poisson ratio (so when expanded in one direction, they contract in the other direction) (Figure 1.2b). In addition to this model, these structures have also been made from a silicone elastomer, Zhermack Elite Double 8. This shows that they indeed exhibit the expected properties, when they are created.

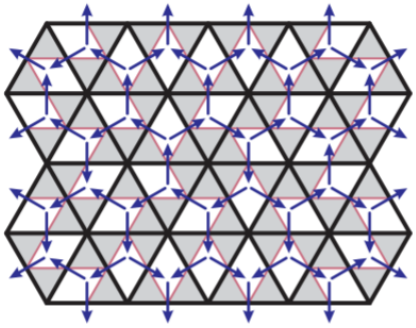

(a) *Structure with negative Poisson's ratio. When it is expanded in the vertical direction, it will also expand in the horizontal direction.*

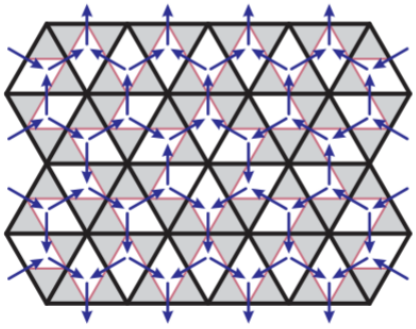

(b) *Structure with positive Poisson's ratio. When this is expanded in the vertical direction, it will contract in the horizontal direction.*

Figure 1.2: *Structures with a predefined Poisson's ratio [9].*

Of course, we can make many more of these structures, with other spin configurations. For example, the spins on the edges of the structure can be alternating or have any other pattern. Also the spins inside the structure do not have to be pointing in the directions shown in 1.2, their directions can be changed as well. From this follows that there are a lot more combinations that can be considered. The problem I will be addressing in this thesis, is to calculate the number of different structures that can be made, by only using the unit cells that have been used in Kettenis' thesis. These structures are also used to create the above tilings and will be defined in

the next section.

1.2 Defining the tiles

First of all, we will give the definition of a plane tiling and tiles, which will be used extensively in this thesis. For a reference, see [10].

Definition 1.2.1. *A* plane tiling *is a countable family of closed sets* $\mathcal{T} = \{T_1, T_2, ...\}$, *of which the union* $\bigcup T_i$ *is the whole plane (in general* $\mathbb{R}^2$*), and for which the interiors are non-intersecting, i.e. for the interiors* T_i° *and* T_j° *of* T_i *and* T_j *respectively, we have:* $T_i^\circ \cap T_j^\circ = \emptyset$, *for all* $T_i, T_j \in \mathcal{T}$.

Definition 1.2.2. $T_1, T_2, ...$ *are called the* tiles *of* $\mathcal{T}$.

For now, we will assume that the plane we are looking at, is a subspace of $\mathbb{R}^2$, and not the whole of $\mathbb{R}^2$.

We will consider a plane tiling on a subspace of $\mathbb{R}^2$, where every tile is congruent to the tile depicted in Figure 1.3. Every tile is thus congruent to a triangle consisting of two smaller triangles and one rhombus.

This tile can be rotated, so that there are three different options for the tile that can be chosen for every location of the tiling. Note that, since we are considering a triangular tiling, these tiles are alternately rotated over an angle equal to π, to be able to place the tiles in the tiling.

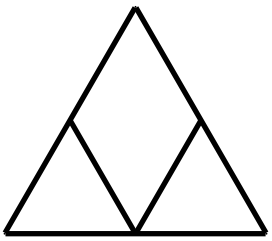

Figure 1.3: *Tile, used for the tiling. Every tile is congruent to this one, the only difference is due to rotation and contraction or extension.*

Taking the beams, having half the length of the edges of the big triangle, to be rigid, and the connection points to be perfect hinges, we find that the tiles can be deformed by exerting some external (contracting or extending) force on the sides of the triangle, so that the system starts to hinge.

Since the beams are rigid, the only way the tiles can be changed, is by increasing or decreasing the size of the rhombus, thus deforming to one of the configurations shown in Figure 1.4. If the size of the rhombus increases, we say the triangle is expanded, if the size of the rhombus decreases, we say that the triangle is contracted.

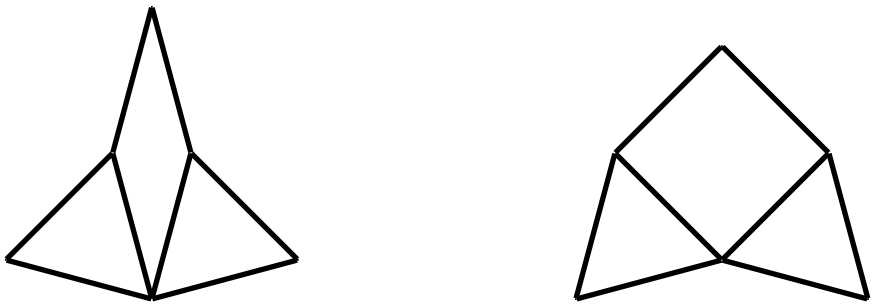

(a) *Contracted triangle* ***(b)*** *Expanded triangle*

Figure 1.4: *Different configurations, to which the tile can transform.*

Instead of considering the triangles to be hinging, we can also represent this movement with spins on the edges of the triangles, as is done in Figure 1.5. Consider the contracted triangle. The two sides that are moving inwards, will be represented by the spins that are pointing inwards, while the spin that is pointing outwards represents the side that is moving outwards. Equivalently we get for the extended triangle, that the two sides that are moving outwards are represented by the spins that are pointing outwards, and the other side, that is moving inwards is represented by the spin that is pointing inwards.

(a) *Simplified contracted unit cell* ***(b)*** *Simplified extended unit cell*

Figure 1.5

This above assignment of spins gives a representation that is easier to analyse. This representation considers the triangles to be rigid, but with the assignation of the spins, that are entering or leaving the triangles on

the edges. To summarise, there are the following constraints on the spins entering or leaving the triangle:

- Two spins point into the triangle and one spin points out; or
- Two spins point out of the triangle, and one spin points in.

This relation between the spins will be referred to as a "two in-one out, or two out-one in" relation, since these are the only two deformed states a single triangle can be in. This gives the two different tiles, as depicted in Figure 1.5.

Now, we can construct a tiling, by placing more of these tiles next to each other. For this, the following conditions have to be satisfied.

- Two tiles have at most 1 edge and 2 vertices in common with each other. This can of course also be only one vertex.
- If 2 tiles have one edge in common, then the associated spins should be pointing in the same direction. If this is not the case, we call the tiling frustrated.

If these triangles are placed in such a way that the tiling is not frustrated, then a feasible hingeable tiling can be constructed.

Something important we have to keep in mind, is what we will call the "invariance principle". This principle gives that reversing all of the spins on a particular subset of the edges, which we will call the "invariant subset", will not change the number of feasible configurations. Note that only the spins on the invariant subset are given, all other spins still have to be defined. This property will be proven for some of the considered configurations in Theorems 3.2.1, 4.3.3 and 4.3.4. Of course, it is also possible to determine this property by calculating both the number of all feasible configurations for some tiling with predefined edges, and the number of feasible configurations when these spins are reversed. Obviously, this will not be the most efficient way to be able to prove the principle, but it might at least give a general idea about how the principle works.

Chapter 2

Theory

This section will give a general overview of related problems and give an explanation on the problem itself. These related problems have equivalent properties, but are not the same. The chapter is arranged in the following way.

In the first section, we will discuss the 3D variant of the 2D tiling problem we will be studying, as can be found in [11]. It will be shown, that these 3D structures, called voxels, have properties, which the 2D triangles do not possess. After this, we will consider the dual graphs of the triangular lattice, and give an overview of the results found in other literature using this dual graph. In the last section, the goal of this thesis will be discussed, and also some notation will be introduced. Besides this a simple example will be given, as a clarification of the used notation.

2.1 Analogous problem in 3D: voxels

Coulais [11] has been working on 3d structures, called "voxels", forming cubic unit cells. These voxels can be contracted and extended along one of the axes, and they will then extend and shrink along both of the other axes, respectively. Note that in this case there thus are two direction in which the system is contracted and extended, and one direction in which the system is extended and contracted, respectively. In this way, we can also define a "two in-one out, or two out-one in" relation. Here, the three possible unit cells, with for each of them both their contractile and extensive behaviour, are represented in Figure 2.1.

These voxels can be put next to each other, in such a way that when the side of one voxel is expanding, the neighbouring side of an other voxel,

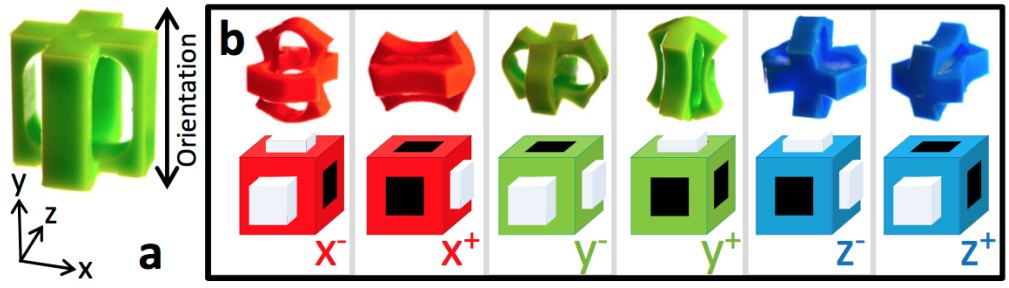

Figure 2.1: *The six voxels, that can be defined using extension and contraction along one of the axes, while the other axes are contracted and extended [11].*

has to be contracted, so that the system can move freely, and no frustration occurs. In this way, 3D tilings of these voxels can be constructed. For any cube of $L \times L \times L$ voxels, the number of distinct feasible spin configurations has been determined in [11], using these 6 voxels as the building blocks. A schematic representation of these numbers is given in Figure 2.2.

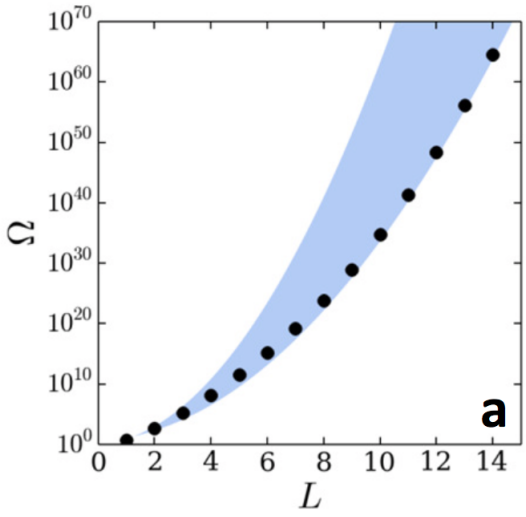

Figure 2.2: *Schematic representation of the number of different $L \times L \times L$ spin configurations. The blue region corresponds to the region between the upper and lower bounds [11].*

The voxels can be viewed as the three-dimensional version of a "two in-one out, or two out-one in" relation, as already explained. There are either two axes along which the voxel extends, while it contracts in the other direction, or there are two axes along which the voxel contracts, while it extends along the other axis. For the triangle this same reasoning holds

for the sides. There are either two sides along which the triangle extends, while it is contracted in the other direction, or there are two sides along which the triangle contracts, while it is extended in the other direction. From this follows that the triangles and the voxels have a similar relevant property.

An upper boundary for the number of feasible configurations for any $L \times L \times L$ cube is given by 3^{L^3}. Namely: every voxel can have 3 possible configurations, and in total there are L^3 voxels in a bigger cube, that is of length $L \times L \times L$. Due to occurrence of frustration, a lot of these 3^{L^3} configurations are not possible. As discussed in [11], the maximum number of feasible configurations for the big cubes can be reduced, due to holographic ordering, thus resulting in 2^{3L^2} feasible configurations. In this case, holographic ordering means that the boundary spins determine all of the inside of the cubes. This is due to the fact that each row of spins has to be alternating, since if the spin is pointing out of the cube on one side, then it also has to be pointing out of the cube on the other side. From this the boundary of the large cube is giving restrictions on the whole interior. These alternating rows of spins also imply that the system is periodic.

What is different for the 2D version of the tiling we are considering, is that on average there are multiple possibilities to place a triangle in a location of the tiling, because in this case, there is no constraint that the arrows alternately have to be pointing into one direction and then in the other. If we want to place a new triangle in a tile, there can be multiple options for this, depending on the already placed triangles. From this follows, that in the triangular 2D case, there is no occurrence of holographic projection, but then there also is no periodicity.

2.2 The ice model

In the ice models a directed graph is considered, to model the distribution of hydrogen atoms in water. As explained in this section, this type of problems uses spins to model the behaviour of the system. The analysis of this problem happens through the use of a directed graph, that can be seen as the dual version of our representation. In this section, the dual graph will be explained, we will give a explanation of the ice model and a summary of the solved versions of the ice model will be given.

Instead of the problem defined in Section 1.2, we can consider the dual version of this problem. Let the tiling with the spins removed be an undi-

rected graph, where the nodes correspond to the vertices of the triangles and the edges to the edges of the triangles. For this undirected graph, we could look at the dual graph. The dual graph is defined as follows, see [12] for a reference.

Definition 2.2.1. *Let a planar undirected graph $G = (V, E)$ be given. Construct a graph $G^* = (V^*, E^*)$, for which each node $v^* \in V^*$ corresponds to a region of the graph G. If two of the regions r_i, r_j are adjacent, then the nodes $v_i^*, v_j^* \in G^*$ corresponding to these regions have to be connected. This has to be done in such a way, that the edges of G^* are crossing the edge between those two regions in G only once and that all the edges are non-intersecting. The in this way constructed graph G^* is called the* dual graph *of G.*

For example, if we have the graph, depicted in Figure 2.3, with the black nodes and the solid lines, we can define its dual by the graph depicted with the white nodes and the dashed lines.

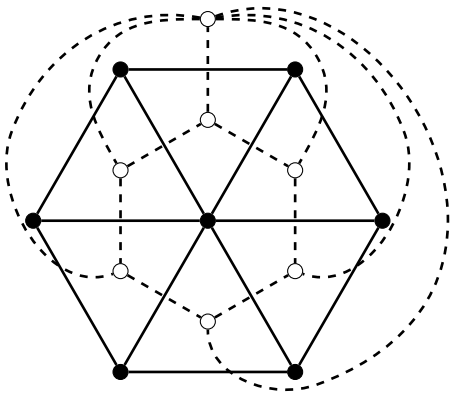

Figure 2.3: *The hexagon, together with its dual graph. The black dots and the solid lines form the original graph, the white dots and dashed lines form the dual graph. Note that all the nodes corresponding to the interior regions have degree 3, while the node that corresponds to the outer region has a degree, equal to the number of triangles adjacent to the unbounded region.*

For the dual graph of the hexagon, every node, that does not correspond to the unbounded region, has 3 neighbours. If we now assign a directed arrow to all of the edges between the nodes so that the edges are directed, we get a one-to-one correspondence between the assignment of the directed arrows and the problem defined in Section 1.2. This "dual" problem again has to satisfy the constraint, that for the nodes corresponding to the interior regions, there either have to be two arrows pointing into

this node, or two arrows leaving this node, while the other is going into the remaining direction. From this follows that the in-degree of these nodes either need to be 1 or 2, from which follows that the out-degree is equal to 2 or 1, respectively. The last node, corresponding to the outer region, does not have to satisfy these properties.

For this dual version a related problem is defined. This problem is the ice model, as defined by Pauling [13]. Here, a consideration of the number of feasible configurations is given for the orientation of water molecules in ice in 3D, where some conditions are imposed on these structures. These conditions are as follows:

- for each of the oxygen atoms that is being considered, there are two hydrogen atoms that are attached to the oxygen atom, at distances of 0.95 Å, so forming a water molecule. Assumed is that the angle of the HOH configuration is about 105°, like it is in the gas molecule;
- each water molecule is oriented in such a way that the two hydrogen atoms are pointing in the direction of two of the four surrounding oxygen atoms, thus forming hydrogen bonds;
- approximately one hydrogen atom lies on the axis of oxygen-oxygen bonds, due to the orientation of the water molecules;
- if two molecules are not adjacent, under normal conditions, no element of one of these molecules has an influence on the configuration of the other molecule.

An orientation of these ice molecules is shown in Figure 2.4a.

As explained by Lieb [15], the ice model described above can be considered as a square lattice model in 2D, where each of the vertices of the lattice has 4 neighbours. On each of the edges of the lattice a spin is placed, that is either directed towards the vertex, or towards the neighbour, as shown in Figure 2.4b. Now there must be two spins, pointing into each vertex, as well as 2 spins pointing out. First Pauling [13] gave a rough estimate of the number of possibilities, for a large number N of vertices in the lattice, namely: $W = \left(\frac{3}{2}\right)^N$. Lieb [15],[16] solved the problem of finding the exact number of configurations, using the method of the transfer matrix, yielding the value: $W = \left[\left(\frac{4}{3}\right)^{\frac{3}{2}}\right]^N = \left(\frac{4}{3}\right)^{\frac{3}{2}N}$. There are other models related to the ice model, which are called ice-type models. These models are

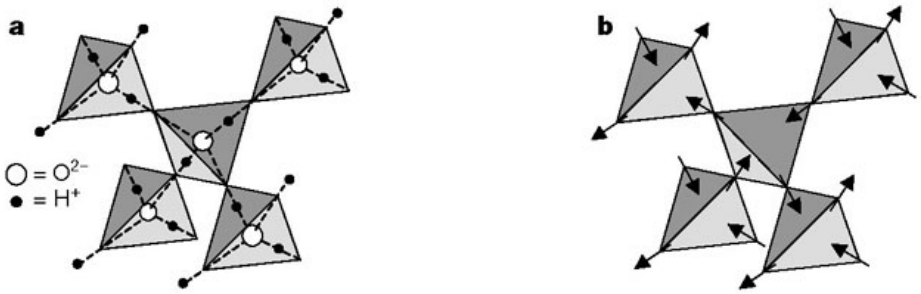

(a) *Representation of the Ice model, where the nodes are the oxygen atoms, and on the edges the hydrogen atoms are placed. Each of the hydrogen atoms has to be closer to one of the oxygen neighbours. Every oxygen atom needs two hydrogen atoms that are closer to this oxygen atom than to the neighbouring oxygen atoms of the oxygen atom.*

(b) *Spin representation of the Ice model. Each spin corresponds to a hydrogen atom, and is pointing towards an oxygen atom if the hydrogen atom is closer to this oxygen atom. Each oxygen atom needs two spins pointing into this atom, and two out of it.*

Figure 2.4: *[14].*

for example the F model of Rys [17], and the Slater KDP model [18]. In these two models specific spin configurations of the spins are made more likely, by giving them an energy equal to 0, while all of the other spin configurations have the same positive energy. Both these models have been solved by Lieb [19], [20]. Wu [21] considered a modified version of the Rys F model of an antiferroelectric. Here, two kinds of doubly ionized vertices are added to the already existing six different possibilities for the edges. In this paper, only for a particular choice of energies for the vertices, a closed form of the partition function was provided.

A generalization of ice-type models is the eight-vertex model, where also sink and source vertices are included. This problem was solved by Baxter [22], in the case of zero energy for all of the vertices. Additionally, Baxter gave the partition function for the Rys F model on a triangular lattice and found a solution for the case where a restriction is imposed on the probabilities of the various types of vertices [23].

However, for none of these ice-type models a lattice model has been considered, where each of the vertices, that does not represent the infinite region, is connected to three other vertices, as in the dual graph of

our problem. Therefore, as far as we know, the number of configurations has not been calculated for this problem. Since this calculation is an interesting thing to consider, this thesis will be about finding the numbers of configurations for the tilings.

2.3 Goal of this thesis and notation

In this thesis, we will consider the number of ways these triangles can be placed, such that the tiling defined in Section 1.2 is hingeable and not frustrated when it is deformed. As explained on page 6, a tiling is not frustrated if for each pair of triangles that have one edge in common, the associated spins on this edge are pointing in the same direction.

We will say that two tilings are different, if the spin pattern, the way the spins are placed on the edges of the tiles, of these tilings are different. A spin pattern is different if there are (one or more) triangles in the pattern, having one or more spins on their edges that are reversed, compared to the other spin pattern. From this follows, that for the two tilings the deformation under some load will look different. We will not take into account rotational symmetries, i.e. if two tilings are the same under a rotation, but different when they are not rotated, they will also be considered different. The extension and contraction of a tiling result in a different spin pattern on the edges, therefore these will be counted as two different configurations.

The tiling that we will consider mostly in this thesis consists of k rows and l triangles per row, which we will call a (k, l)-tiling. In general, we will call the number of feasible configurations for a structure with k rows of l triangles $a_{(k,l)}$. The simplest example is a single row consisting of l triangles. It is quite easy to derive the number of feasible configurations for this case. This is what will be done in 2.3.1.

Example 2.3.1. We will compute the number of configurations that are possible for a $(1, n)$-tiling, a tiling consisting of one row of tiles, as depicted in Figure 2.5. This row can iteratively be built up, namely: The first tile can be chosen out of 6 possible ones (3 expanding, 3 contracting, which can be found by rotating the tiles in Figure 1.5). For adding all of the next tiles apart from this first one, one of the sides has to be fixed, so for these tiles 3 configurations can be chosen. From this we find that the number of feasible configurations is equal to

$$a_{(1,n)} = 6 \cdot 3^{n-1} = 2 \cdot 3^n. \tag{2.1}$$

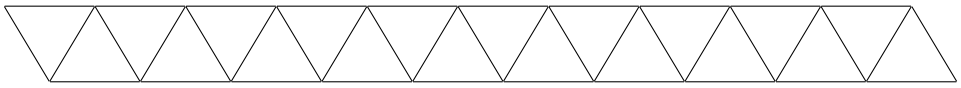

Figure 2.5: *A row of 20 tiles*

In example 2.3.1, we can already find an application of the invariance principle. If we for example know what the first triangle looks like, we get that there are 3^n feasible configurations. Now reversing the spins in this first triangle, will also give the same number of configurations. From this we find that the first triangle is an invariant subset. In the same way, we can take all different spin configurations on all the edges of this tiling, and show that these form an invariant subset.

Chapter 3

Hexagonal Tilings

One of the tilings that is the easiest to consider, apart from the single row that has been studied in Section 2.3, is the hexagon. The analysis of the hexagon will show, that in spite of it being a small lattice, it already has a large amount of feasible configurations. For this hexagon, the number of feasible configurations can be calculated easily by considering all the possibilities. To get a feeling for finding the number of feasible configurations, we will perform the calculation to find the number of feasible configurations in this chapter.

3.1 The hexagon

The hexagonal tiling consists of six triangular tiles, that are placed in such a way, that they have one side in common with two of the other tiles. The intersection of these six triangles is only one point, see also Figure 3.1.

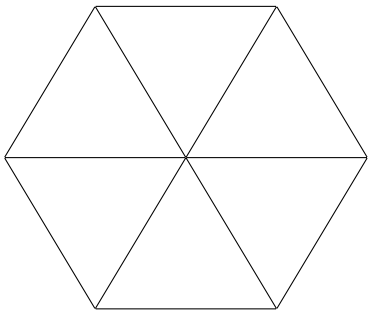

Figure 3.1: *General form of the hexagon, where no spins are included.*

3.2 Calculating the number of configurations in a hexagon

We will calculate the number of feasible configurations for the hexagonal tiling, shown in Figure 3.1. For this we will first prove an invariance principle, using the spins in the interior of the hexagon–which we will call the inner spins–as the invariant subset. We will use these inner spin configurations, to determine the number of configurations for the spins on the boundary–to which we will refer as the outer spins–and thus calculate the number of feasible configurations.

Theorem 3.2.1. *The inner spins of the hexagon form an invariant subset.*

Proof. Let some inner spin configuration of the hexagon be given. For this spin configuration, there may be outer spins, for which only one spin assignment is possible. This is the case if the two inner spins on the edges of the triangle are both pointing inwards or both pointing outwards. If this is not the case, the inner edges of this triangle have one spin pointing in and one pointing out, so that the direction of the outer spin in this triangle can be chosen.

If we would now reverse all of the spins on the inside of the hexagon, we know that again, the same amount of outer spins has to be fixed. This is due to the fact that for each triangle, that had two spins pointing in, the two spins are now pointing out of this triangle, so that the outer spin now has to be pointing in. In the same way, we find that all of the spins that were pointing out of the triangle are now pointing in, thus the outer spin has to be pointing out. Apart from this, we know that if a triangle had one spin pointing in and one spin pointing out, there will now again be one spin pointing in and one pointing out, thus the direction of the outer spin can still be chosen, so that the amount of outer spins that can be chosen stays the same.

Since both the number of outer spins that can be chosen and the number of outer spins of which the direction is fixed stay the same, we also find that the total number of configurations, when the inner spin configuration is reversed stays the same. This value is namely equal to 2 to the power of the number of the sides that can be chosen. From this follows that the invariance principle holds if we take the inner spins of the hexagon as the invariant subset. □

First, a tiling will be considered where the inner spins point counterclockwise. After this, we will subsequently reverse more of these inner

spins and make them point clockwise. For all of these inner spin configurations, the number of configurations for the spins on the boundary of the hexagon will be calculated. Adding these up will give the total number of feasible configurations. From the invariance principle follows that it is sufficient to consider half of the cases, because the other half is found in the same way.

Out of convenience, the inner spins that are reversed, will be coloured blue, and the spins on the boundary of the hexagon of which the direction is fixed by spins inside the hexagon, will be coloured red.

When all of the inner spins point counter-clockwise, the outer spins can point either in or out of every one of the six triangles, see Figure 3.2.

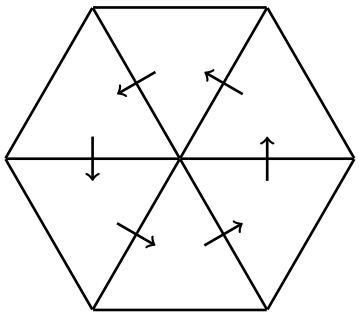

Figure 3.2: *Hexagon, where all spins are pointing counter-clockwise.*

This results in 2^6 configurations. Note that when all spins are reversed, so they are all pointing clockwise, the invariance principle shows that this number will be the same. Thus when all spins are pointing in the same direction (either clockwise or counter-clockwise), there in total are $2 \cdot 2^6$ configurations.

If precisely one spin points clockwise, we know that two of the outer spins are fixed (Figure 3.3a). The direction the other four outer spins point in, can still be chosen.

In the same way, for two up to five inner spins that are pointing clockwise, but are next to each other (so there is no counter-clockwise spin in between), there are only two fixed outer spins, see also Figure 3.3b, hence there are four outer spins that can be chosen. Note that there are five ways to choose the number of clockwise inner spins and 6 rotations, so in total there are $6 \cdot 5$ different ways in which the four outer spins of which the

direction can be chosen, can be placed. In total, we find $6 \cdot 5 \cdot 2^4$ feasible configurations, for the outer spins in these cases.

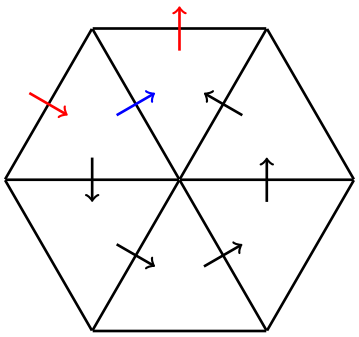

(a) *Hexagon, where only one inner spin is pointing clockwise, all other inner spins are pointing counter-clockwise. Here, two of the outer spins are determined.*

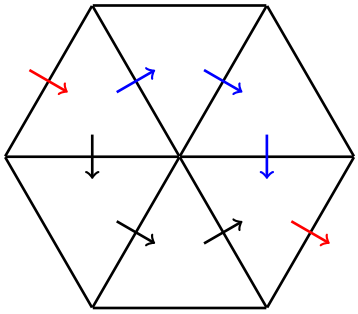

(b) *Hexagon, where three inner spins next to each other are pointing clockwise, and three inner spins (also next to each other) are pointing counter-clockwise. Again, two of the outer spins are determined.*

Figure 3.3

If we now have two non-adjacent groups of non-consecutive clockwise inner spins, we know that four of the outer spins have to be fixed, so only two can be chosen. For these groups the feasible combinations of configurations are: -one plus one reversed spin; -two plus one reversed spins; -two plus two reversed spins; -or one plus three reversed spins. Considering these different cases give the following situations.

- Two groups both consisting of one clockwise pointing inner spin: Let the first clockwise inner spin be placed randomly, then we can choose the second clockwise inner spin to be placed in one of the three edges that is non-adjacent to the edge of the first reversed inner spin. For two of these cases (Figure 3.4a), we can rotate over 6 angles, to get different configurations. For the last case (Figure 3.4b) only three rotations can be applied. This gives us $3 \cdot 2^2 + 6 \cdot 2^2 = 9 \cdot 2^2$ feasible configurations.

- Suppose there is one group of two clockwise inner spins, and one group of one clockwise inner spin. Let the two reversed inner spins be placed randomly. The single clockwise spin can not be chosen in an edge adjacent to the two clockwise spins. Hence, there are two

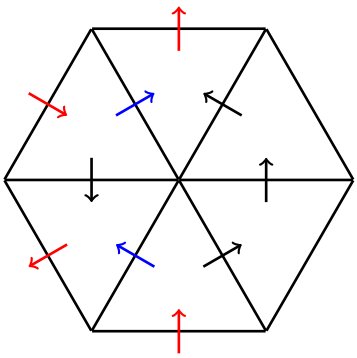

(a) *Hexagon, where the two clockwise inner spins are positioned in such a way that there is one counterclockwise inner spin in between on one side and three on the other side.*

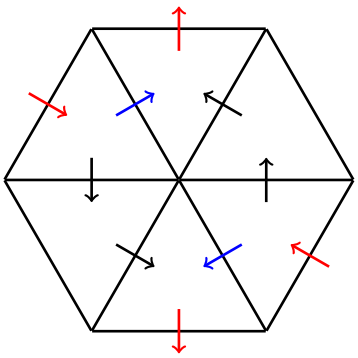

(b) *Hexagon, where the two clockwise inner spins are positioned in such a way that there are 2 counterclockwise inner spins in between on both sides.*

Figure 3.4

possibilities for the location of this spin (see Figure 3.5a and Figure 3.5b). Due to rotations, there are $6 \cdot 2 \cdot 2^2$ feasible configurations for this case.

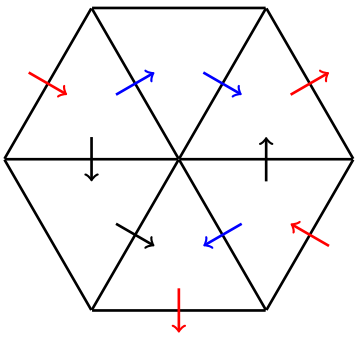

(a)

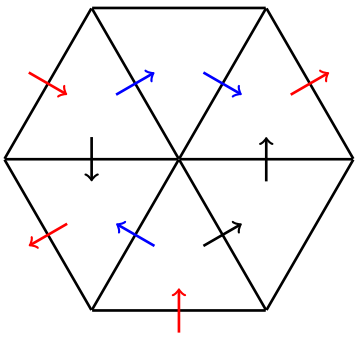

(b)

Figure 3.5: *Hexagons, with a group of two inner spins pointing clockwise and a group of a single inner spin pointing clockwise. If the group of two spins is fixed, in the two highest edges of the hexagon, then the position of the single reversed inner spin can be chosen. This inner spin has to be in a side that is not adjacent to the first two, and can thus be chosen in two ways, as depicted in Figures 3.5b and 3.5a.*

- For the two plus two case, we always need to have two single inner spins opposite of each other, that are not reversed, so there are $3 \cdot 2^2$

feasible configurations, as follows with the invariance principle, and one of the cases of the hexagon with two groups of one inner spin pointing clockwise.

- If there are three plus one inner spins that are pointing clockwise, reversing all of the spins, will give the second case of the hexagon with two groups of one inner spin pointing clockwise. Thus follows with the invariance principle that there are $6 \cdot 2^2$ feasible configurations.

From this follows, that in total, there are 30×2^2 feasible configurations for two pairs of non-consecutively reversed inner spins.

When we have three groups of non-consecutively clockwise pointing inner spins, we know that there has to be one spin pointing clockwise, one pointing counter-clockwise, again one pointing clockwise and so on, see Figure 3.6a. All of the spins are now fixed, as well as the position of the reversed spins. There is only one rotation (Figure 3.6b), that can be used to find another configuration, thus finding a total number of configurations, equal to: $2 \cdot 1$.

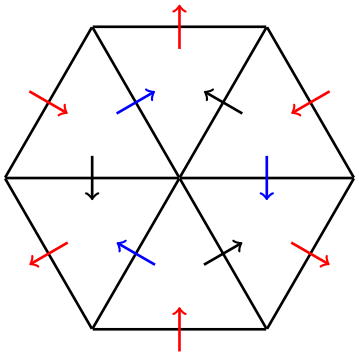

(a) *Hexagon, where three pairs of single spins are reversed, thus forming an alternating pattern of clockwise and counter-clockwise spins.*

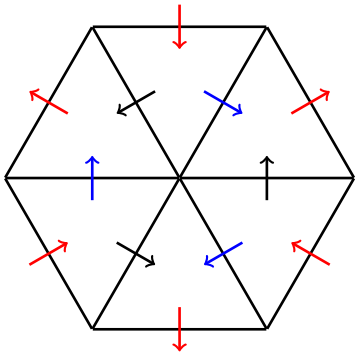

(b) *Hexagon, that can be obtained by rotating 3.6a over* $60°$, $180°$ *or* $300°$.

Figure 3.6

In total, we thus find a number of configurations, equal to:

$$\#\text{ configurations for hexagon} = 2 \cdot 2^6 + 30 \cdot 2^4 + 30 \cdot 2^2 + 2 \cdot 1 = 730.$$

3.3 Number of flows entering or leaving the hexagonal cell

As we can see in the cases in Section 3.2, the number of spins entering the hexagon is equal to the number of triangles that have two spins pointing in and one spin pointing out of the hexagon. Equivalently, the number of spins leaving the triangle is equal to the number of triangles that have two spins pointing in and on spin pointing out. This holds for all of the hexagons, we will prove this.

Theorem 3.3.1. *The number of outer spins pointing out of and into the hexagon is equal to the number of triangles that have two spins pointing out and one in and two spins pointing in and one out, respectively.*

Proof. Let x be the number of triangles, that have two spins pointing out of them and one in, and y be the number of triangles with two spins pointing in and one spin pointing out of them.

Since every spin pointing out has a spin on the adjacent triangle that is pointing in, we know that for these triangles there are six spins in the interior of the hexagon, that are pointing out of any of the triangles and six that are pointing into the triangles. Thus the total number of spins that is pointing out of the six triangles, has to be equal to $6 + \#\{\text{spins pointing out of the hexagon}\}$. Note that this number is also equal to $2x + y$, since there are x triangles with two spins pointing out and y triangles with one spin pointing out. Thus: $2x + y = 6 + \#\{\text{spins pointing out of the hexagon}\}$ and equivalently $x + 2y = 6 + \#\{\text{spins pointing into the hexagon}\}$. Subtracting the second equation from the first, will give that $x - y = \#\{\text{spins pointing out of the hexagon}\} - \#\{\text{spins pointing into the hexagon}\}$.

Further, the triangles with two spins pointing out and one in and the hexagons with two spins pointing in and one out are the only possibilities, thus we have that they have to sum up to 6, so $x + y = 6$. Hence: $2x = 6 + \#\{\text{spins pointing out of the hexagon}\} - \#\{\text{spins pointing into the hexagon}\} = 2 \cdot \#\{\text{spins pointing out of the hexagon}\}$, since the number of spins pointing out and into the hexagon add up to 6. Now we have $x = \#\{\text{spins pointing out of the hexagon}\}$ and $y = \#\{\text{spins pointing in the hexagon}\}$. □

Chapter 4

General Tilings

In this chapter, we will present a way to calculate the number of feasible configurations for a tiling of k rows, each consisting of l triangles. We will first derive a formula for the number of configurations for a $(2, l)$-tiling, a tiling consisting of 2 rows that each have l triangles, using $(2, 2)$-tilings as building blocks. This is done, to serve as an easy example of the method of derivation, that will be used in the next sections.

Then we will present a derivation of the number of configurations for any $(k, 2)$-tiling with given boundary spins on the left and right boundaries, that will be used as the building blocks for (k, l)-tilings. With this derivation, we can formulate an algorithm to calculate the number of configurations for the (k, l)-tilings.

Finally, we will present a numerical algorithm, that is implemented in Python, to calculate the numbers of feasible configurations, This algorithm gives the same results as the theoretical derivation in the first four sections.

4.1 Calculating the number of configurations for a (2,2)-tiling

First of all, we will consider a $(2, 2)$-tiling, that can be used to iteratively build the $(2, l)$-tiling. For this single layer, the number of different configurations will be calculated, given that both the left and right boundaries have a given spin configuration.

To derive these numbers, we will consider the 16 possible $(2, 2)$-tilings with given boundary spins on the left and right side and calculate the number of feasible configurations in these cases, as shown in Figure 4.1. The equal sign between the pairs is because of the invariance principle,

using the left as right boundary as invariant subset, which will be proven for the more general case of a $(k, 2)$-tiling in Theorem 4.3.3.

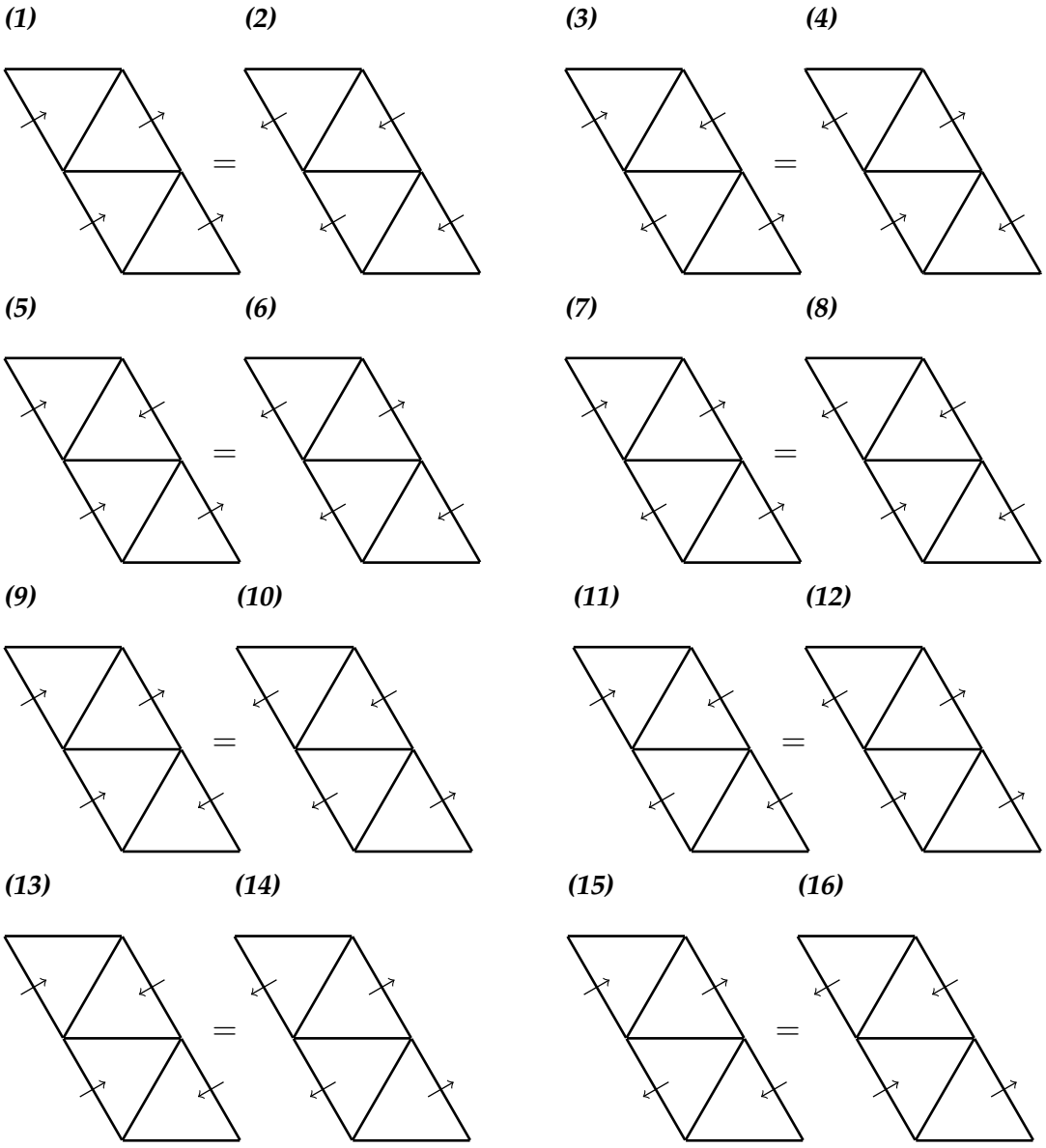

Figure 4.1: *The different feasible configurations for the 2 by 2 tiling. Tilings that are the same under the invariance principle (which will be proven in 4.3.3), are placed with an equal sign between them.*

We will consider tiling (1) and calculate the number of feasible configurations for this case. For the other tilings the computation is similar.

We will colour the inner edges of the tiling, to let the derivation be more unambiguous, and assign spins to these edges and the upper and lower boundary. This is done in the way shown in Figure 4.2.

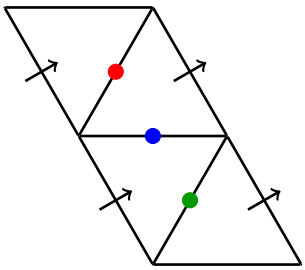

Figure 4.2: *The configuration for the first tiling. To both the coloured edges and the upper and lower edge of the tiling, we will assign spins and count the number of different ways this can be done.*

This gives the following cases.

- Taking the spin at the red location to be pointing to the lower-right side, will give a choice for the spin on the blue edge.
  - The spin on the blue side can be pointing down, which then implies that the spin on the green side has to be pointing to the lower-right side. This gives the configuration shown in Figure 4.3. We can now choose both the configurations of the upper and lower edge, thus in this case we get 4 configurations.

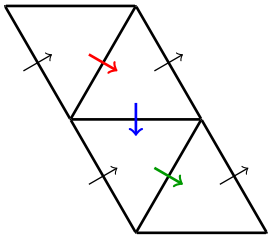

Figure 4.3: *Configuration for the second case, in which the red spin is pointing to the lower-right side, the blue spin is pointing down, and the green spin has to be pointing to the lower-right side as well.*

  - The blue spin can be pointing up. Then the green spin can be chosen freely. If the green spin is pointing to the upper-left side (Figure 4.4a), we can only choose the spin on the upper edge,

thus getting 2 configurations. If the green spin is pointing into the lower-right side (Figure 4.4b), the spin on the lower edge can also be chosen. This results in 4 feasible configurations.

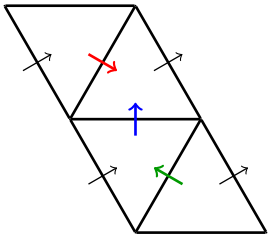

(a) *Configuration for the first case, where the red spin is pointing to the lower-right side, the blue spin is pointing up and the green spin is pointing to the upper-left side.*

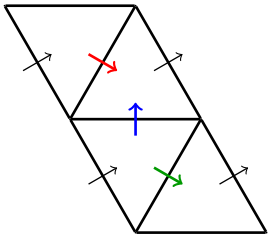

(b) *Configuration for the first case, where the red spin is pointing to the lower-right side, the blue spin is pointing up and the green spin into the lower-right side.*

Figure 4.4

- For the next case, we take the spin on the red edge to be pointing into the upper-left side. Then the spin on the blue side has to be pointing up. The direction of the spin on the green side can still be chosen freely. We can now have this spin to be pointing to the upper-left side (Figure 4.5a).

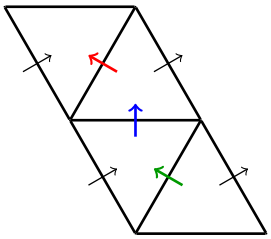

(a) *Configuration, where the red spin is pointing to the upper-left side, the blue spin is pointing up and the green spin is pointing into the upper-left side.*

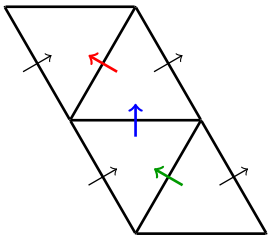

(b) *Configuration, where the red spin is pointing to the upper-left side, the blue spin is pointing up and the green spin is pointing into the lower-right side.*

Figure 4.5

If this is the case, both spins on the upper and lower edge can not be chosen freely, thus there is only one feasible configuration. The

green spin can also be pointing to the lower-right side (Figure 4.5b). Then the direction of the spin on the lower side can still be chosen, thus giving two configurations.

In total, we thus get 13 configurations. We have listed the other tilings with predefined edges in Figure 4.6. These numbers have both been simulated and determined with the brute force calculation described above.

tiling		number of config.	tiling		number of config.
(1), (2)	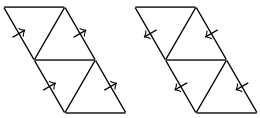	13	(9), (10)	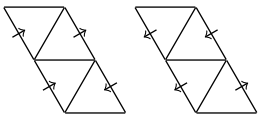	11
(3), (4)	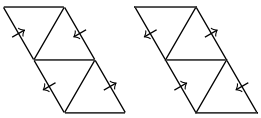	10	(11), (12)	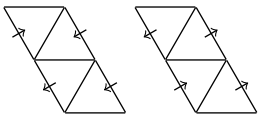	11
(5), (6)	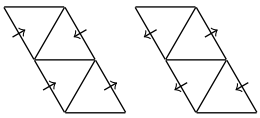	9	(13), (14)	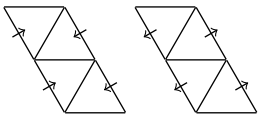	6
(7), (8)	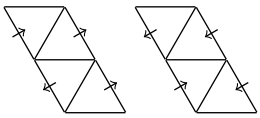	9	(15), (16)	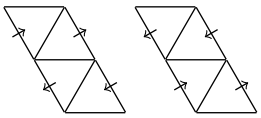	12

Figure 4.6: *Number of feasible configurations for the possible 2-by-2 tilings, with predefined edges on the left and right side.*

From the above we can conclude, that there are 19 feasible configurations, where the spins on the left side are both pointing to the right, and the spins on the right side are pointing into the same direction (case (1) and (13)), just like when the spins on the left side are pointing to the left, and the spins on the right side are pointing in the same direction (case (2) and (14)).

If the spins on the left side would both be pointing to the right or both to the left, and the spins on the right side would both be pointing in a

different direction, there would be 20 feasible configurations (case (5) and (9)) or (case (6) and (10)). Thus, if the spins on the left boundary are both pointing to the left, this gives that in total there are 39 feasible configurations.

In the same way we can also derive for the left boundary that when these spins are both pointing in an opposite direction, while on the right boundary they are both pointing in the same direction, this gives 20 feasible configurations (case (7) and (11) or case (8) and (12)). When the spins on the left boundary are both pointing in a different direction, and also the spins on the right boundary are pointing in a different direction, this gives 22 feasible configurations (cases (3) and (15) or (4) and (16)). Now, we get that when the two spins on the left boundary are pointing in a different direction, the number of feasible configurations is equal to 42.

As in Section 2.3, we will call $a_{(k,l)}$ the number of configurations that are feasible for a tiling of k rows, consisting of l triangles. Because l is even in all of these cases discussed here, we will write $n = \frac{l}{2}$, where n is an integer. With the invariance principle we can let $a^1_{(2,2n)}$ and $a^2_{(2,2n)}$ be the number of feasible configurations for a $(2, 2n)$-tiling, for which the spins on the left side of the tiling are pointing in the same direction (either to the left or the right) and in a different direction (either the first one is pointing to the right and the second to the left or vice versa), respectively. The total number of feasible configurations can then be found with the formula: $a_{(2,2n)} = 2 \cdot (a^1_{(2,2n)} + a^2_{(2,2n)})$.

4.2 Putting (2,2)-tilings next to each other

A tiling of two rows, with $2(n-1)$ triangles per row, can be extended to a tiling of two rows, with $2n$ triangles per row. This can be done by putting a $(2, 2)$-tiling next to this first tiling. Of course, the spins on the left side of the $(2, 2(n-1))$-tiling have to correspond to the spins on the right side of the $(2, 2)$-tiling. Therefore, for every spin configuration on the left side of the $(2, 2(n-1))$-tiling, there is a fixed number of configurations for the $(2, 2)$-tiling that can be placed on the left of the $(2, 2(n-1))$-tiling. The possible number of configurations that can be added has been calculated in Section 4.1.

We will consider the tiling of 2 rows with $2n$ triangles in one row, where on the left side both spins are pointing inwards. There are four possibilities for the left side of the $(2, 2(n-1))$-tiling, to which the $(2, 2)$-tiling will be

attached. Indeed, these spins can point in the same direction (either to the left or to the right) or they can point into a different direction. This results in the 4 cases shown in Figure 4.7.

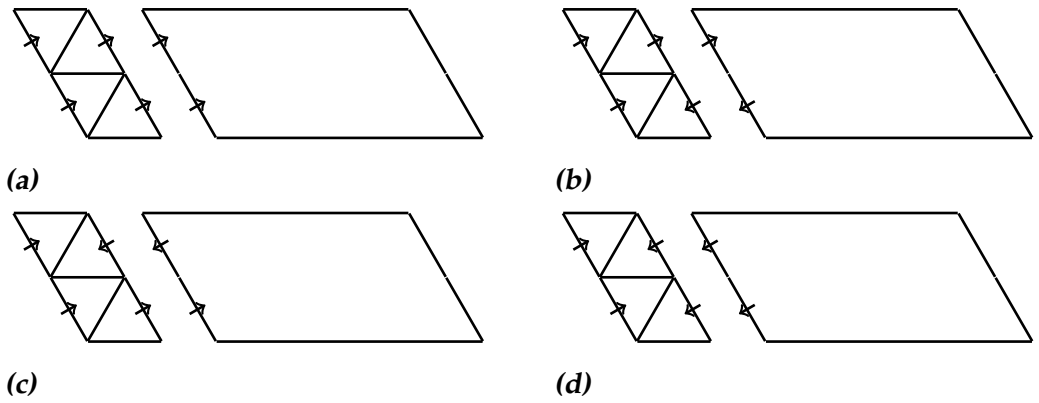

Figure 4.7: *The 4 cases for the orientation of the $(2, 2(n-1))$-tiling and the right side of the $(2,2)$-tiling, given the that the spins on the left boundary of the $(2,2)$-tiling are both pointing inwards. This $(2,2)$-tiling can then be attached to the $(2, 2(n-1))$-tiling to form a $(2, 2n)$-tiling, with a predefined boundary on the left side of the tiling.*

Because of the invariance principle for the left boundary of a $(k, 2n)$-tiling, which will be proven in Theorem 4.3.4, we only have to consider one of the cases where both spins are pointing in the same direction and one where the spins are pointing in a different direction. For this, we will use the configurations where the first spin on the left boundary is pointing to the right, so we have to consider the odd elements in Figure 4.6. Also, with this invariance principle for the left boundary of a $(k, 2n)$-tiling, we know that the number of configurations $a^1_{(2,2(n-1))}$ for the $(2, 2(n-1))$-tiling in Figure 4.7a is equal to the number of configurations for the $(2, 2(n-1))$-tiling in Figure 4.7d. In the same way, also the number of feasible configurations $a^2_{(2,2(n-1))}$for the $(2, 2(n-1))$-tiling in Figure 4.7b can be found to be equal to the number of configurations for the $(2, 2(n-1))$-tiling in Figure 4.7c.

For the case shown in Figure 4.7a, we know that for the $(2,2)$-tiling, there are 13 feasible configurations, while for the $(2, 2(n-1))$-tiling, there are $a^1_{(2,2(n-1))}$ feasible configurations. In total, there thus are $13 \cdot a^1_{(2,2(n-1))}$ feasible configurations. The cases in Figures 4.7b, 4.7c and 4.7d, equivalently give $11 \cdot a^2_{(2,2(n-1))}$, $9 \cdot a^2_{(2,2(n-1))}$ and $6 \cdot a^1_{(2,2(n-1))}$ feasible configu-

rations, respectively. In total, the number of configurations for the $(2, 2n)$-tiling, where both spins are pointing to the right, thus equals:

$$a^1_{(2,2n)} = 19 \cdot a^1_{(2,2(n-1))} + 20 \cdot a^2_{(2,2(n-1))}. \tag{4.1}$$

Equivalently, for the case that the first spin on the left side of the $(2, 2n)$-tiling is pointing to the right, while the second is pointing to the left, we can derive the following recurrence relation for the number of feasible configurations:

$$a^2_{(2,2n)} = 20 \cdot a^1_{(2,2(n-1))} + 22 \cdot a^2_{(2,2(n-1))}. \tag{4.2}$$

This can be written in a matrix. Using the recurrence relations give:

$$\begin{pmatrix} a^1_{(2,2n)} \\ a^2_{(2,2n)} \end{pmatrix} = \begin{pmatrix} 19 & 20 \\ 20 & 22 \end{pmatrix} \cdot \begin{pmatrix} a^1_{(2,2(n-1))} \\ a^2_{(2,2(n-1))} \end{pmatrix} = \begin{pmatrix} 19 & 20 \\ 20 & 22 \end{pmatrix}^{n-1} \cdot \begin{pmatrix} a^1_{(2,2)} \\ a^2_{(2,2))} \end{pmatrix}$$

We know that $a^1_{(2,2)} = 19 + 20 = 39$, and $a^2_{(2,2)} = 20 + 22 = 42$, since all elements of the first $(2, 2)$-tiling for which the spins on the left side have a certain direction can be added, because the right side of these tiles do not matter, when the tiling is extended. From this we find:

$$\begin{pmatrix} a^1_{(2,2n)} \\ a^2_{(2,2n)} \end{pmatrix} = \begin{pmatrix} 19 & 20 \\ 20 & 22 \end{pmatrix}^{n-1} \cdot \begin{pmatrix} 39 \\ 42 \end{pmatrix}. \tag{4.3}$$

Now we will analyse the properties of this matrix, to derive the number of feasible configurations from this. Let $A = \begin{pmatrix} 19 & 20 \\ 20 & 22 \end{pmatrix}$. The characteristic polynomial of A is:

$$\begin{aligned} \det(\lambda I - A) = \det \begin{pmatrix} \lambda - 19 & -20 \\ -20 & \lambda - 22 \end{pmatrix} &= (\lambda - 19)(\lambda - 22) - 400 \\ &= \lambda^2 - 41\lambda + 18. \end{aligned}$$

The eigenvalues and the eigenvectors of A are:

$$\lambda_{1,2} = \frac{41 \pm \sqrt{(41)^2 - 72}}{2} = \frac{41 \pm \sqrt{1609}}{2}$$

and

$$v_{1,2} = \begin{pmatrix} -3 \pm \sqrt{1609} \\ 40 \end{pmatrix}.$$

This results in $A = PDP^{-1}$, where:

$$D = \begin{pmatrix} \frac{41-\sqrt{1609}}{2} & 0 \\ 0 & \frac{41+\sqrt{1609}}{2} \end{pmatrix}, \quad P = \begin{pmatrix} -3-\sqrt{1609} & -3+\sqrt{1609} \\ 40 & 40 \end{pmatrix}$$

and

$$P^{-1} = \frac{1}{128720} \cdot \begin{pmatrix} 40\sqrt{1609} & 1609+3\sqrt{1609} \\ -40\sqrt{1609} & 1609-3\sqrt{1609} \end{pmatrix}$$

Multiplying A^n with $\begin{pmatrix} a^1_{(2,2)} \\ a^2_{(2,2)} \end{pmatrix}$ gives – using $\alpha = 41+\sqrt{1609}$ and $\bar{\alpha} = 41-\sqrt{1609}$:

$$\begin{aligned} \begin{pmatrix} a^1_{(2,2n)} \\ a^2_{(2,2n)} \end{pmatrix} &= A^{n-1} \begin{pmatrix} a^1_{(2,2)} \\ a^2_{(2,2)} \end{pmatrix} = PD^{n-1}P^{-1} \begin{pmatrix} a^1_{(2,2)} \\ a^2_{(2,2)} \end{pmatrix} \\ &= \frac{2^{-n-1}}{1609} \begin{pmatrix} (1609-37\sqrt{1609})\bar{\alpha}^n + (1609+37\sqrt{1609})\alpha^n \\ (1609-43\sqrt{1609})\bar{\alpha}^n + (1609+43\sqrt{1609})\alpha^n \end{pmatrix}. \end{aligned} \tag{4.4}$$

With the relation $a_{(2,2n)} = 2\left(a^1_{(2,2n)} + a^2_{(2,2n))}\right)$, we get that the number of feasible configurations for a $(2,2n)$-tiling, $n \in \{1,2,...\}$, is given by (again with $\alpha = 41+\sqrt{1609}$ and $\bar{\alpha} = 41-\sqrt{1609}$):

$$a_{(2,2n)} = 2^{-(n-1)} \left((1 - \frac{40}{\sqrt{1609}})\bar{\alpha}^n + (1 + \frac{40}{\sqrt{1609}})\alpha^n \right). \tag{4.5}$$

Note that, since n is an integer, for the above cases, we used the fact that $l = 2n$ is even.

It is also possible to derive a relation for the case that the number of triangles in a row is odd. Note that for any general tiling with k rows of triangles, k triangles are added on the left or right side of the $(k, l-1)$-tiling, which all have 3 possible configurations (as can be seen in Figure 4.8). The number of configurations for a tiling with an odd number l of triangles in one row is thus equal to: $a_{(k,l)} = 3^k \cdot a_{(k,l-1)}$. Thus, for a $(2, 2n+1)$-tiling with n integer, the following relation holds:

$$a_{(2,2n+1)} = 3^2 \cdot 2^{-n+1} \left((1 - \frac{40}{\sqrt{1609}})\bar{\alpha}^n + (1 + \frac{40}{\sqrt{1609}})\alpha^n \right). \tag{4.6}$$

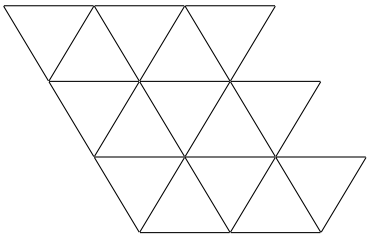

Figure 4.8: *A tiling of 3 rows, each containing 5 triangles. Note that, for the last triangle in a row, (if there is an odd number of triangles in every row), there are always 3 feasible configurations, independently of the other parts of the tiling.*

4.3 Derivation of the matrices

In this section, we will derive a way to calculate the numbers of feasible configurations for any $(k, 2)$-tiling, a tiling consisting of k rows, each having 2 triangles in one row. From these values, it is possible to derive the number of configurations for any larger (k, l)-tiling. This is done by again considering a matrix with all of the possible amounts of configurations, where each of the elements of the matrix is giving the amount of configurations for each given left and right boundary. Then again the total number of feasible configurations can be determined by applying matrix multiplication.

To this end, we first determine the elements of a $(1, 2)$-unit tiling, as depicted in Figure 4.9. After this, we will iteratively built up a $(k-1, 2)$-tiling with given spins on the left and right boundary, by adding unit tilings, for which the left and right boundary are given, on the lower side of a $(k-1, 2)$-tiling (also with given spins on the left and right boundary) and determine the number of possibilities. The reason why we need to keep track of the spin configurations on the left and right boundary of the $(k, 2)$-tiling, is that we need to be able to place the $(k, 2)$-tilings next to each other in such a way, that the sides correspond.

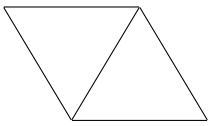

Figure 4.9: *(1,2)- unit tiling, used to construct tilings of k rows of 2 triangles, which in its turn can be used to construct a tiling of k rows of l triangles.*

There are 4 possible positions for the outer spins, that can be varied to get different configurations. These 4 positions are the left, right, top and

bottom of the unit cell. We thus have $2^4 = 16$ different possibilities for the configurations on the boundaries. In Figures 4.10 - 4.13 these possibilities are discussed and the different amounts of configurations are given.

1. If the spin on the left is pointing to the left and the spin on the right is pointing to the right, we get the different cases and numbers of feasible configurations that are given in Figure 4.10.

Spin orientation	Number of configurations	Spin orientation	Number of configurations
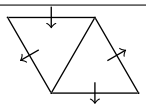	1	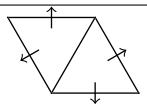	0
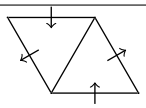	2	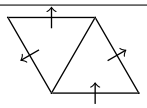	1

Figure 4.10: *Number of configurations for the given spin orientations. Here, the left spin is pointing to the left and the right spin is pointing to the right.*

2. If the spin on the left is pointing to the right and the spin on the right is pointing to the left, we get the number of feasible configurations, given in Figure 4.11.

Spin orientation	Number of configurations	Spin orientation	Number of configurations
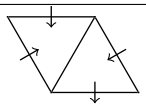	1	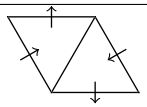	2
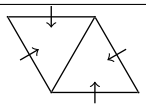	0	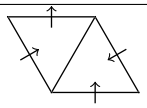	1

Figure 4.11: *Number of configurations for the given spin orientations. Here, the left spin is pointing to the right, while the right spins is pointing to the left.*

3. If both spins on the left and right are pointing to the right, we get the number of feasible configurations, that are given in Figure 4.12.

4. If both spins on the left and right are pointing to the left, we get the number of configurations, given in Figure 4.13.

Spin orientation	Number of configurations	Spin orientation	Number of configurations
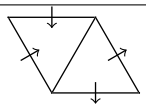	1	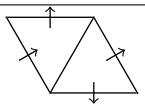	1
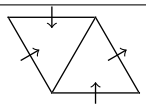	1	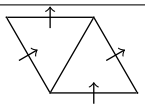	2

Figure 4.12: *Number of configurations for the given spin orientations. Here, the left and right spins are both pointing to the right.*

Spin orientation	Number of configurations	Spin orientation	Number of configurations
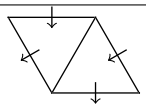	2	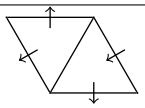	1
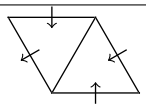	1	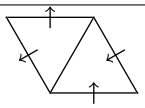	1

Figure 4.13: *Number of configurations for the given spin orientations. Here, the left and right spins are both pointing to the left.*

To build up a $(k, 2)$-tiling, we need keep in mind the spin orientations of the left and right boundary of the tiling. Therefore, we will have the vector $c_k = (c_k(l), c_k(r)) \in (-1, 1)^k \times (-1, 1)^k$, to keep track of the left and right boundaries. Let $\mathcal{C}_k$ be the collection of all these c_k, so

$$\mathcal{C}_k = \left\{ c_k = (c_k(l), c_k(r)) \in (-1, 1)^k \times (-1, 1)^k \right\}.$$

Both $c_k(l)$ and $c_k(r)$ are vectors of length k, and the i-th element of these vectors represents the direction of the spins of the unit cell at height i, seen from above, of the left and right side respectively, of the $(k, 2)$-tiling. If this value is 1, then the spin at this location is pointing to the right, if it is -1, then the spin is pointing to the left.

Example 4.3.1. If $(c_k(l))_i = 1$, then the spin at height i of the left boundary of the $(k, 2)$-tiling is pointing to the right.

Consider $k = 3$ with $c_3 = (c_3(l), c_3(r)) = \left(\begin{pmatrix} 1 \\ 1 \\ -1 \end{pmatrix}, \begin{pmatrix} -1 \\ 1 \\ -1 \end{pmatrix} \right)$. Then the tiling is as depicted in Figure 4.14.

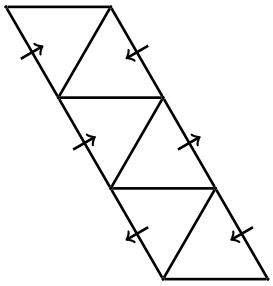

Figure 4.14: *The (3,2)-tiling, with the $c_k(l)$ and $c_k(r)$, as described in Example 4.3.1.*

Now some notation will be introduced. Denote by $a_{(k,2)}(c_k)$ the number of configurations for a $(k,2)$-tiling, for which the spins on the left and right boundary are given by c_k. Furthermore, denote by $a^1_{(k,2)}(c_k)$ and $a^2_{(k,2)}(c_k)$ the number of these configurations that have their spin on the lower side pointing down and up, respectively. Note that we do not use the invariance principle here, so we do consider all of the configurations independently. From this, we find that

$$a_{(k,2)}(c_k) = a^1_{(k,2)}(c_k) + a^2_{(k,2)}(c_k).$$

Using these configurations, we can again determine the number of feasible configurations iteratively, by attaching a $(1,2)$-unit tiling to the lower side of the $(k-1,2)$-tiling.

We then have the following possible iterations:

- When the k-th element added to the tiling, has its spin on the left pointing to the left and on the right its spin pointing to the right, we get $(c_k)_k = ((c_k(l))_k, (c_k(r))_k) = (-1,1)$. To find c_k, $c_{k-1}(l)$ has to be extended by one element to a vector of length k, with the last element equal to -1 and $c_{k-1}(r)$ has to be extended by one element to a vector of length k, with the last element equal to 1. That is $c_k = \left(\begin{pmatrix} c_{k-1}(l) \\ -1 \end{pmatrix}, \begin{pmatrix} c_{k-1}(r) \\ 1 \end{pmatrix}\right)$.

  With this reasoning and Table 4.10, we know that:

$$a^1_{(k,2)}(c_k) = a^1_{(k-1,2)}(c_{k-1})$$

and

$$a^2_{(k,2)}(c_k) = 2a^1_{(k,2)}(c_{k-1}) + a^2_{(k,2)}(c_{k-1}),$$

with $a^1_{(1,2)}((-1,1)) = 1$ and $a^2_{(1,2)}((-1,1)) = 3$, where we have dropped the brackets of the vector for notational convenience. We will do this every time we have $k = 1$. From this, we can again derive a recurrence relation, when this $(1,2)$-tiling is added as the k-th unit tiling in the column, resulting in Equation 4.7.

$$\begin{pmatrix} a^1_{(k,2)}(c_k) \\ a^2_{(k,2)}(c_k) \end{pmatrix} = \begin{pmatrix} 1 & 0 \\ 2 & 1 \end{pmatrix} \cdot \begin{pmatrix} a^1_{(k-1,2)}(c_{k-1}) \\ a^2_{(k-1,2)}(c_{k-1}) \end{pmatrix}, \text{ for } k \geq 2, \tag{4.7a}$$

and

$$\begin{pmatrix} a^1_{(1,2)}((-1,1)) \\ a^2_{(1,2)}((-1,1)) \end{pmatrix} = \begin{pmatrix} 1 \\ 3 \end{pmatrix}. \tag{4.7b}$$

- When the k-th added element has the spins on the left pointing to the right, and the spin on the right side pointing to the left, the k-th element of c_k is equal to $(c_k)_k = ((c_k(l))_k, (c_k(r))_k) = (1,-1)$. If we add an unit tiling with the arrows pointing inwards to a $(k-1,2)$-tiling, we thus know that $c_k(l)$ has to be extended with an element 1, and $c_k(r)$ has to be extended with an element -1. Then we get $c_k = \left(\begin{pmatrix} c_{k-1}(l) \\ 1 \end{pmatrix}, \begin{pmatrix} c_{k-1}(r) \\ -1 \end{pmatrix}\right)$. Hence using Table 4.11,

$$\begin{pmatrix} a^1_{(k,2)}(c_k) \\ a^2_{(k,2)}(c_k) \end{pmatrix} = \begin{pmatrix} 1 & 2 \\ 0 & 1 \end{pmatrix} \cdot \begin{pmatrix} a^1_{(k-1,2)}(c_{k-1}) \\ a^2_{(k-1,2)}(c_{k-1}) \end{pmatrix}, \text{ for } k \geq 2, \tag{4.8a}$$

and

$$\begin{pmatrix} a^1_{(1,2)}(((1),(-1))) \\ a^2_{(1,2)}((1,-1)) \end{pmatrix} = \begin{pmatrix} 3 \\ 1 \end{pmatrix}. \tag{4.8b}$$

- When the element that is added at the k-th position, has its spins on the left and right side both pointing to the right, the k-th element of c_k is: $(c_k)_k = ((c_k(l))_k, (c_k(r))_k) = (1,1)$. This implies $c_k = \left(\begin{pmatrix} c_{k-1}(l) \\ 1 \end{pmatrix}, \begin{pmatrix} c_{k-1}(r) \\ 1 \end{pmatrix}\right)$ and Table 4.12 yields the recurrence relation:

$$\begin{pmatrix} a^1_{(k,2)}(c_k) \\ a^2_{(k,2)}(c_k) \end{pmatrix} = \begin{pmatrix} 1 & 1 \\ 1 & 2 \end{pmatrix} \cdot \begin{pmatrix} a^1_{(k-1,2)}(c_{k-1}) \\ a^2_{(k-1,2)}(c_{k-1}) \end{pmatrix}, \text{ for } k \geq 2, \tag{4.9a}$$

and

$$\begin{pmatrix} a^1_{(1,2)}\left(\left((1),(1)\right)\right) \\ a^2_{(1,2)}\left((1,1)\right) \end{pmatrix} = \begin{pmatrix} 2 \\ 3 \end{pmatrix}. \tag{4.9b}$$

- Finally, when the spins on the left and right side of the k-th added element are both pointing to the left, the k-th element of c_k is equal to $(c_k)_k = ((c_k(l))_k, (c_k(r))_k) = (-1,-1)$. Thus we find that $c_k = \left(\begin{pmatrix} c_{k-1}(l) \\ -1 \end{pmatrix}, \begin{pmatrix} c_{k-1}(r) \\ -1 \end{pmatrix}\right)$ and Table 4.13 yields:

$$\begin{pmatrix} a^1_{(k,2)}(c_k) \\ a^2_{(k,2)}(c_k) \end{pmatrix} = \begin{pmatrix} 2 & 1 \\ 1 & 1 \end{pmatrix} \cdot \begin{pmatrix} a^1_{(k-1,2)}(c_{k-1}) \\ a^2_{(k-1,2)}(c_{k-1}) \end{pmatrix}, \text{ for } k \geq 2, \tag{4.10a}$$

and

$$\begin{pmatrix} a^1_{(1,2)}\left((-1,-1)\right) \\ a^2_{(1,2)}\left(\left((-1),(-1)\right)\right) \end{pmatrix} = \begin{pmatrix} 3 \\ 2 \end{pmatrix}. \tag{4.10b}$$

As soon as we know the order of the spins of one tiling, we can determine the number of configurations, that is possible.

Example 4.3.2. Let $k = 5, l = 2$, with the directions of the spins on the boundaries, from top to bottom: both spins to the right, left spin to the left and right spin to the right, left spin to the right and right spin to the left, both spins to the left and both spins to the right, see also Figure 4.15.

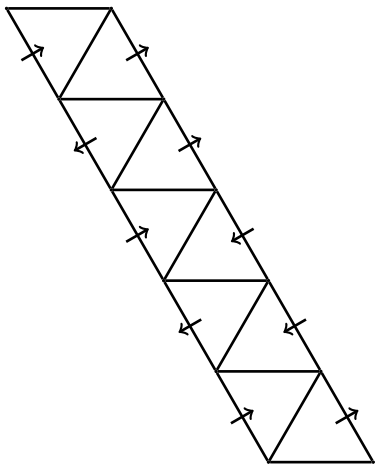

Figure 4.15: *The (5,2)-tiling, with the configurations of the spins from top to bottom: right, outwards, inwards, left and right.*

Now we have that

$$c_5 = \left(\begin{pmatrix} 1 \\ -1 \\ 1 \\ -1 \\ 1 \end{pmatrix}, \begin{pmatrix} 1 \\ 1 \\ -1 \\ -1 \\ 1 \end{pmatrix} \right),$$

so that:

$$\begin{aligned} \begin{pmatrix} a^1_{(5,2)}(c_5) \\ a^2_{(5,2)}(c_5) \end{pmatrix} &= \begin{pmatrix} 1 & 1 \\ 1 & 2 \end{pmatrix} \cdot \begin{pmatrix} a^1_{(4,2)}(c_4) \\ a^2_{(4,2)}(c_4) \end{pmatrix} = \ldots \\ &= \begin{pmatrix} 1 & 1 \\ 1 & 2 \end{pmatrix} \cdot \begin{pmatrix} 2 & 1 \\ 1 & 1 \end{pmatrix} \cdot \begin{pmatrix} 1 & 2 \\ 0 & 1 \end{pmatrix} \cdot \begin{pmatrix} 1 & 0 \\ 2 & 1 \end{pmatrix} \cdot \begin{pmatrix} a^1_{(1,2)}(c_1) \\ a^2_{(1,2)}(c_1) \end{pmatrix} \\ &= \begin{pmatrix} 1 & 1 \\ 1 & 2 \end{pmatrix} \cdot \begin{pmatrix} 2 & 1 \\ 1 & 1 \end{pmatrix} \cdot \begin{pmatrix} 1 & 2 \\ 0 & 1 \end{pmatrix} \cdot \begin{pmatrix} 1 & 0 \\ 2 & 1 \end{pmatrix} \cdot \begin{pmatrix} 2 \\ 3 \end{pmatrix} \\ &= \begin{pmatrix} 62 \\ 85 \end{pmatrix}, \end{aligned} \tag{4.11}$$

where

$$c_4 = \left(\begin{pmatrix} 1 \\ -1 \\ 1 \\ -1 \end{pmatrix}, \begin{pmatrix} 1 \\ 1 \\ -1 \\ -1 \end{pmatrix} \right), c_3 = \left(\begin{pmatrix} 1 \\ -1 \\ 1 \end{pmatrix}, \begin{pmatrix} 1 \\ 1 \\ -1 \end{pmatrix} \right),$$

$$c_2 = \left(\begin{pmatrix} 1 \\ -1 \end{pmatrix}, \begin{pmatrix} 1 \\ 1 \end{pmatrix} \right) \text{ and } c_1 = (1, 1)\,.$$

Thus, the number of configurations with the spins oriented as in Figure 4.15, is equal to $62 + 85 = 147$, where 62 is the number of elements with boundary conditions c_k and the spin on the lower side pointing out, and 85 is this same number, but with the spin on the lower side pointing in.

We will now prove the invariance theorem for a $(k, 2)$-tiling, when the invariant subset consists of the left and right boundaries of the tiling. In terms of the c_k, this gives:

$$a_{(k,2)}((c_k(l), c_k(r)) = a_{(k,2)}((-c_k(l), -c_k(r)).$$

This means for a given spin configuration c_k on the left and right boundaries, that the number of feasible configurations equals the number of feasible configurations, with the spins on the left and the right boundaries reversed.

Theorem 4.3.3. *(Invariance principle for $(k,2)$-tiling with left and right boundary as invariant subset.)*
For a $(k,2)$-tiling, we have:

$$a_{(k,2)}((c_k(l),c_k(r)) = a_{(k,2)}((-c_k(l),-c_k(r)).$$

Proof. Assume a tiling with left boundary $c_k(l)$ and right boundary $c_k(r)$ is given. The number of feasible configurations $a_{(k,2)}(c_k)$ can be determined by multiplying the matrices, in the iterative way described above. Note that if we reverse all of the spins on both the left and the right boundary, so if we look at the tiling with boundary $(-c_k(l),-c_k(r))$, then the rows and columns of all of these matrices, that we had to multiply, will be interchanged. This is due to the fact that when the spins were pointing outwards, they will now point inwards, and the matrix corresponding to these spins pointing outwards is exactly the one where the spins are pointing inwards, but where the rows and columns are interchanged. If we now multiply the resulting matrices, we will get the same result as the one found above, but only with the two elements in the row of the final vector interchanged. Adding these values up, will give the same result as found when the spins were pointing in the opposite direction. □

For any $(k,2n)$-tiling, we will use Theorem 4.3.3 and induction to n to derive that the number of feasible configurations when the spins on the left side are fixed is equal to the number of feasible configurations, when all these fixed spins are reversed. For this we will use the following notation: $a_{(k,2n)}(c_k(l))$ is the number of configurations where the left boundary is given by $c_k(l)$.

Theorem 4.3.4. *(Invariance principle for $(k,2n)$-tiling with left boundary as invariant subset.)*
For a $(k,2n)$-tiling, we have:

$$a_{(k,2n)}(c_k(l)) = a_{(k,2n)}(-c_k(l)).$$

Proof. For $n=1$, we know that $a_{(k,2)}(c_k(l)) = \sum_{c_k(r)} a_{(k,2)}((c_k(l),c_k(r))$. As shown in Theorem 4.3.3, we have

$$a_{(k,2)}((c_k(l),c_k(r)) = a_{(k,2)}((-c_k(l),-c_k(r)).$$

For this last number of configurations, we know that $a_{(k,2)}(-c_k(l)) = \sum_{c_k(r)} a_{(k,2)}((-c_k(l),-c_k(r))$ holds. Thus we find

$$\begin{aligned} a_{(k,2)}(c_k(l)) &= \sum_{c_k(r)} a_{(k,2)}((c_k(l),c_k(r)) \\ &= \sum_{c_k(r)} a_{(k,2)}((-c_k(l),-c_k(r)) = a_{(k,2)}(-c_k(l)). \end{aligned}$$

Let $N \in \mathbb{N}_{\geq 2}$ be given, and assume that the statement holds for $n < N$. We will prove that it also holds for N.

Note that we can write the number of elements for any spin configuration $c_k(l)$ on the left boundary as follows:

$$a_{(k,2N)}(c_k(l)) = \sum_{c_k(r)} a_{(k,2)}((c_k(l), c_k(r))a_{(k,2(N-1))}(c_k(r)).$$

Because of Theorem 4.3.3, we find:

$$a_{(k,2)}((c_k(l), c_k(r)) = a_{(k,2)}((-c_k(l), -c_k(r)).$$

With the induction hypothesis follows for any $(k, 2(N-1))$-tiling, that:

$$a_{(k,2(N-1))}(c_k(r)) = a_{(k,2(N-1))}(-c_k(r)),$$

where $c_k(r)$ again the left boundary of the $(k, 2(N-1))$-tiling. Hence, we find that

$$\begin{aligned} a_{(k,2N)}(c_k(l)) &= \sum_{c_k(r)} a_{(k,2)}((c_k(l), c_k(r))a_{(k,2(N-1))}(c_k(r)) \\ &= \sum_{c_k(r)} a_{(k,2)}((-c_k(l), -c_k(r))a_{(k,2(N-1))}(-c_k(r)) \\ &= a_{(k,2N)}(-c_k(l)) \end{aligned}$$

Thus the theorem holds for any $n \geq 1$. □

As given above, let $a_{(k,2n)}(c_k(l))$ be the number of feasible $(k, 2n)$-tilings which have a left boundary $c_k(l)$. The number of feasible configurations can be calculated, using

$$a_{(k,2n)}(c_k(l)) = \sum_{c_k(r)} a_{(k,2)}((c_k(l), c_k(r))a_{(k,2(n-1))}(c_k(r)). \tag{4.12}$$

To do this, all of the numbers $a_{(k,2)}((c_k(l), c_k(r))$ need to be calculated, to construct a matrix A_k. This matrix can be used to iteratively determine the number of feasible configurations for a $(k, 2n)$-tiling, and contains the different numbers of configurations for a $(k, 2)$-tiling with a left boundary $c_k(l)$, and right boundary $c_k(r)$.

By virtue of the invariance principle of Theorem 4.3.4, we do not need to consider the full matrix of the elements $a_{(k,2)}((c_k(l), c_k(r))$, but we can consider half of the rows, by leaving out all rows, where the first spin on

the left boundary is pointing to the left. Now we only consider all spins configurations on the left boundary, where the first spin is pointing to the right. With the invariance principle then follows, that the total number of configurations can be found, by multiplying the number found with the above configurations by 2.

In the same way, we can apply the invariance principle of Theorem 4.3.4 to the $(k, 2(n-1))$-tiling. Since $a_{(k,2(n-1))}(c_k(r)) = a_{(k,2(n-1))}(-c_k(r))$, it is possible to take the two numbers of feasible configurations $a_{(k,2(n-1))}(c_k(l), c_k(r))$ and $a_{(k,2(n-1))}(c_k(l), -c_k(r))$ together into one element of the matrix. Thus the matrix A_k can be constructed as a 2^{k-1}-by-2^{k-1}-matrix.

To construct this matrix, we will first introduce the subset $C_k(l) \subset \mathcal{C}_k$ by

$$C_k(l) = \{c_k \in \mathcal{C}_k | (c_k(l))_1 = 1\},$$

so these are spin configurations on the left boundary with the first spin pointing to the right. These elements already give half of the configurations for the spin on the left side and we find

$$\mathcal{C}_k \setminus C_k(l) = \{c_k \in \mathcal{C}_k | (c_k(l))_1 = -1\}.$$

This makes sure the amount of rows is reduced to 2^{k-1}, and we are considering all the spin configurations on the left boundary, where the first spin is pointing to the right. Now let

$$C_k(l, r_1) = \{c_k \in \mathcal{C} | (c_k(l))_1 = 1, (c_k(r))_1 = 1\},$$

and

$$C_k(l, r_{-1}) = \{c_k \in \mathcal{C} | (c_k(l))_1 = 1, (c_k(r))_1 = -1\}$$

be the collection of spin configurations that have the first spin on the left boundary pointing to the right, and the first spin on the right boundary to the right and left, respectively. Then the number of columns can be reduced by taking the elements $c_{k_1} \in C_k(l, r_1)$ and $c_{k_{-1}} \in C_k(l, r_{-1})$, such that $c_{k_1}(r) = -c_{k_{-1}}(r)$ together, which can be done, since with the invariance principle of Theorem 4.3.4 follows that

$$\begin{aligned} a_{(k,2(n-1))}(c_{k_1}(r)) &= a_{(k,2(n-1))}(-c_{k_1}(r)) \\ &= a_{(k,2(n-1))}(c_{k_{-1}}(r)) = a_{(k,2(n-1))}(-c_{k_{-1}}(r)). \end{aligned}$$

Example 4.3.2 (Continued). We consider the $2^4 \times 2^4$ matrix, corresponding to the case where $k = 5$, and consider the element in Example 4.3.2. Apart from this element, we will also need the configuration, which we will call

c_5', where the spins on the right boundary are reversed. This gives $c_5' = (c_5'(l), c_5'(r)) = \left(\begin{pmatrix} 1 \\ -1 \\ 1 \\ -1 \\ 1 \end{pmatrix}, \begin{pmatrix} -1 \\ -1 \\ 1 \\ 1 \\ -1 \end{pmatrix} \right)$. By a similar computation as the one applied in Example 4.3.2 we find that this number is equal to 118, so that the matrix element of A corresponding to this case is equal to $147 + 118 = 265$.

Consider the case of k rows in a tiling. Introduce the 2^{k-1}-by-2^{k-1}-matrix, with elements equal to the number of $(k, 2)$-tilings with boundaries $(c_k(l), c_k(r)) \in C_k(l, r_1)$ or $(c_k(l), -c_k(r)) \in C_k(l, r_1)$. To construct the matrix elements, we have to order the left and right boundaries of the $(k, 2)$-tilings. This is done in the following way. For every element a_{ij} of the matrix A_k we consider the binary representation of $i - 1$ and $j - 1$ with k digits. This thus gives us all 2^{k-1} different binary numbers of k digits, that start with a 0. Now we can let these binary numbers correspond to the different assignments of spins on the left and right boundary of the $(k, 2)$-tiling. This is done as follows:

- Let $m \in \{1, 2, ..., k\}$. Consider an element a_{ij} of the matrix A_k. If the binary representation (with k digits) of $i - 1$ has a 0 as m-th digit (counted from the left), then the two configurations corresponding to a_{ij} have the spin on the left boundary at height m pointing to the right. On the other hand, if the m-th digit is a 1, then the configuration corresponding to a_{ij} has the spin on the left boundary at height m pointing to the left.

- Let $n \in \{1, 2, ..., k\}$. Again consider an element a_{ij} of the matrix A_k. Now we look at the columns of this matrix: If the binary representation (with k digits) of $j - 1$ has a 0 as n-th digit (counted from the left), then the configuration corresponding to a_{ij} has the spin on the right boundary at height n pointing to the right. On the other hand, if the n-th digit is a 1, then the configuration corresponding to a_{ij} has the spin on the right boundary at height n pointing to the left.

  The other case we need to build the elements a_{ij} of the matrix A_k is the one where all the spins on the right boundary are reversed. In this case, we thus need that if the binary digit of $j - 1$ is 0, then the configuration corresponding to a_{ij} has the spin on the right boundary at height n pointing to the left, and if this is 1, the spin has to be pointing to the right.

Example 4.3.2 (Continued)**.** For Example 4.3.2, we have for the left side that the first, third and fifth spin are pointing to the right. Thus the binary digit of $i-1$ is 01010, and thus this results in $i-1=10$, so that $i=11$.

Conversely, we will show that we have $j=7$. The binary digit of $j-1=6$ is 00110, hence we need the cases, where the spins on the right boundary that are pointing to the right are the first, second and fifth, while the third and fourth spin are pointing to the left. On the other hand, we then also need the case where the spins on the right boundary are reversed. This is indeed corresponding to the configurations found before in Example 4.3.2.

Now that we know the ordering of the elements of A_k, we can easily determine A_k. This process is shown in Algorithm 1 (where $Bin(i)$ is the binary representation of i, with k digits).

We will apply Algorithm 1 to the case $k=2$.

Example 4.3.5. Let $k=2$. The algorithm gives (we will leave out the subscript $_{(2,2)}$:

$$A_2 = \begin{pmatrix} a\left(\binom{1}{1},\binom{1}{1}\right)+a\left(\binom{1}{1},\binom{-1}{-1}\right) & a\left(\binom{1}{1},\binom{1}{-1}\right)+a\left(\binom{1}{1},\binom{-1}{1}\right) \\ a\left(\binom{1}{-1},\binom{1}{1}\right)+a\left(\binom{1}{-1},\binom{-1}{-1}\right) & a\left(\binom{1}{-1},\binom{1}{-1}\right)+a\left(\binom{1}{-1},\binom{-1}{1}\right) \end{pmatrix}$$
$$= \begin{pmatrix} 13+6 & 11+9 \\ 9+11 & 12+10 \end{pmatrix} = \begin{pmatrix} 19 & 20 \\ 20 & 22 \end{pmatrix}$$

In the same way, we can also derive these matrices, for bigger values of k. This for example gives:

$$A_3 = \begin{pmatrix} 42 & 42 & 44 & 40 \\ 40 & 47 & 49 & 47 \\ 44 & 49 & 53 & 49 \\ 42 & 45 & 49 & 47 \end{pmatrix}.$$

4.4 Configurations with k different from 2

From the matrices derived in the last chapter, it is possible to derive the total number of feasible configurations. First, we have to determine these matrices with the number of feasible configurations, where the boundaries on the left and right sides are fixed. After this, we also need to determine

Algorithm 1 Algorithm to calculate the matrices for the number of feasible configurations for a k by 2 tiling.

1. $a_{ij} = 0$, for i in $1, ..., 2^{k-1}$, j in $1, ..., 2^{k-1}$
2.
for i in $1, ..., 2^{k-1}$ **do**

for j in $1, ..., 2^{k-1}$ **do**

for m in $1, ..., k$ **do**

if $\lfloor \frac{Bin(i-1)}{10^{k-m}} \rfloor (\text{mod } 10) = 1$ **then** $(c_k(l))_m = -1$

else if $\lfloor \frac{Bin(i-1)}{10^{k-m}} \rfloor (\text{mod } 10) = 0$ **then** $(c_k(l))_m = 1$

end if

end for

for n in $1, ..., k$ **do**

if $\lfloor \frac{Bin(j-1)}{10^{k-n}} \rfloor (\text{mod } 10) = 1$ **then** $(c_k(r))_n = -1$

end if

if $\lfloor \frac{Bin(j-1)}{10^{k-n}} \rfloor (\text{mod } 10) = 0$ **then** $(c_k(r))_n = 1$

end if

end for

$(A_k)_{ij} = a_{(k,2)}(c_k(l), c_k(r)) + a_{(k,2)}(c_k(l), -c_k(r))$

end for

end for

the vector with the number of feasible configurations for the first column. Since the right boundary can have any spin configuration, we can add up all elements that have a determined spin configuration on the left boundary, but any spin configuration on the right boundary To get these, we have to sum over the elements in one row. Thus, we obtain the vector, that we want to multiply the matrices with as follows:

$$a_{(k,2)}(c_k)(l) = \sum_{c_k(r)} a_{(k,2)}(c_k(l), c_k(r)).$$

Then we will get the following results:

For $k = 1$:

$$\left(a^1_{(1,2n)}\right) = \left(9\right)^{n-1} \left(9\right).$$

From this we can easily see that

$$a_{(1,2n)} = 2 \cdot a^1_{(1,2n)} = 2 \cdot 9^n = 2 \cdot 3^{2n}.$$

The $k = 2$ case has already been derived in Section 4.2. Also a formula has been derived for this case.

For the $k = 3$ case, we get:

$$\begin{pmatrix} a^1_{(3,2n)} \\ a^2_{(3,2n)} \\ a^3_{(3,2n)} \\ a^4_{(3,2n)} \end{pmatrix} = \begin{pmatrix} 42 & 42 & 44 & 40 \\ 40 & 47 & 49 & 47 \\ 44 & 49 & 53 & 49 \\ 42 & 45 & 49 & 47 \end{pmatrix}^{n-1} \cdot \begin{pmatrix} 168 \\ 183 \\ 195 \\ 183 \end{pmatrix}.$$

To derive the number of feasible configurations for the $(3, 2n)$-tiling, we need to derive the values $a^1_{(3,2n)}, a^2_{(3,2n)}, a^3_{(3,2n)}$ and $a^4_{(3,2n)}$ with matrix multiplication. Now the number of feasible configurations is given by

$$a_{(3,2n)} = 2 \cdot \left(a^1_{(3,2n)} + a^2_{(3,2n)} + a^3_{(3,2n)} + a^4_{(3,2n)}\right).$$

This matrix (and all matrices for larger values of k) have eigenvalues that are both complex and really large. Therefore the derivation of explicit formulae will become very cumbersome, so we will not give these. We will show this for $k = 3$. Here the largest eigenvalue is, using $\beta = 8168346 +$

$i\sqrt{378469655841705}$:

$$\lambda_1 = \frac{187}{4} + \frac{1}{2}\sqrt{\frac{32905}{4} + \frac{2\beta^{1/3}}{3^{2/3}} + \frac{105886}{(3\beta)^{1/3}}} + \frac{1}{2}\sqrt{\frac{32905}{2} - \frac{2\beta^{1/3}}{3^{2/3}} - \frac{105886}{(3\beta)^{1/3}} + \frac{5959611}{4\sqrt{\frac{32905}{4} + \frac{2\beta^{1/3}}{3^{2/3}} + \frac{105886}{(3\beta)^{1/3}}}}}, \quad (4.13)$$

which is approximately equal to 182.763. Assume that the Jordan Normal Form of A_k contains a component in the direction of the eigenvector with the biggest eigenvalue. Then we know, with the properties of the Jordan Normal Form, that with every iteration, the number of configurations has to grow with a factor that is about 182.76. If we consider the ratios between $(3, 2n)$- and $(3, 2(n-1))$-tilings (this we will do in Section 5.1), we can indeed see, that the number of configurations grows with a factor that is about 182.76.

For $k = 4$ we get the following matrix:

$$\begin{pmatrix} a^1_{(4,2n)} \\ a^2_{(4,2n)} \\ a^3_{(4,2n)} \\ a^4_{(4,2n)} \\ a^5_{(4,2n)} \\ a^6_{(4,2n)} \\ a^7_{(4,2n)} \\ a^8_{(4,2n)} \end{pmatrix} = \begin{pmatrix} 99 & 93 & 93 & 78 & 93 & 96 & 88 & 83 \\ 83 & 103 & 103 & 104 & 99 & 108 & 100 & 89 \\ 93 & 99 & 113 & 100 & 113 & 118 & 114 & 99 \\ 78 & 90 & 104 & 106 & 100 & 110 & 106 & 104 \\ 93 & 99 & 109 & 104 & 113 & 118 & 110 & 103 \\ 96 & 108 & 118 & 110 & 118 & 128 & 120 & 108 \\ 88 & 104 & 110 & 106 & 114 & 120 & 116 & 100 \\ 93 & 93 & 99 & 90 & 99 & 108 & 104 & 103 \end{pmatrix}^{n-1} \cdot \begin{pmatrix} 723 \\ 789 \\ 849 \\ 798 \\ 849 \\ 906 \\ 858 \\ 789 \end{pmatrix}.$$

The largest eigenvalue of this matrix is approximately equal to 823.6005. Also here–taking into account the assumption that the Jordan Normal Form contains a component in the direction of the eigenvector with the largest eigenvalue–the number of possible configurations has to grow in every iteration with a factor of about 823.6. This is indeed happening, as will be shown in Section 5.1.

4.5 Calculation

The Python code implemented uses a backtracking algorithm. This means that every time the lattice is completely filled with triangles, the algorithm

will go back to the last triangle that could be changed and change this to a different, not yet considered tiling. The idea of this algorithm, is as follows:

1. Starting from the upper left triangle, fill up the first row with triangles that fit next to each other, then consider the second row, to fill this up, and so on. Triangles can be placed in the tile, if their edges correspond to already placed neighbouring triangles.

2. If no triangle can be added any more, so all of the locations of the tiling are filled, this will be counted as a feasible configuration. Now the algorithm will go back to the last location where a different triangle could have been added that has not been considered before in this location, on its way removing all triangles that have been added after this one. Then the algorithm will take this different triangle and continue with this.

3. If all triangles that can be fitted into a certain location have been considered, the algorithm will again go back to the last location where a different triangle could have been be added and continue with this different triangle.

This will continue until all of the configurations have been considered. Adding all of these feasible configurations, where every location of the tiling is filled with a triangle that has fitting neighbours, will result in the total number of feasible configurations.

The algorithm can be found in Appendix A. In the next chapter, the results of the algorithm can be found.

Chapter 5

Results

For $k \in \{1, 2, ..., 9\}$, and $l \in \{1, 2, ..., 5\}$, we will list the outcomes of the number of configurations, that have been found using both the algorithm and the numerical simulations, that were explained in the last chapter. Also, a discussion on the successive ratios is given. This is first done for a fixed value of l and varying k, and then this is done for a fixed value of k and varying l. The limiting behaviour of these ratios will be discussed and used to derive an estimate for the number of feasible configurations. In the next section, we will study the number of configurations, as a function of the number of spins that point into the tiling at the boundary. After this, we will look at a periodic tiling, and consider the number of spins, of which the direction can be changed, independent of changing any of the other spins.

5.1 Results of calculations (number of feasible configurations)

The number of feasible configurations found, using both the algorithm described in section 4.4, and the numerical simulations in section 4.5, for a (k, l)-tiling, with $k \leq 9$ and $l \leq 5$ are given in Figure 5.1.

Clearly, this table can be extended to larger values of k and l. These numbers can all be found, using the algorithm and simulations, as long as they are not too big (for the computer) to deal with. In Figure 5.2, the number of feasible configurations is plotted as a function of k, for multiple values of l.

For each of these different l, we have made a plot of a continuous function in $\mathbb{R}$, by fitting an exponential function of the form $f(x) = ae^{bx}$ to the

k \ l	1	2	3	4	5
1	6	18	54	162	486
2	36	162	1458	6570	59130
3	216	1458	39366	266454	7194258
4	1296	13122	1062882	10806354	875314674
5	7776	118098	28697814	438264342	106498235106
6	46656	1062882	774840978	17774323650	12957481940850
7	279936	9565938	20920706406	720858511494	1576517564637378
8	1679616	86093442	564859072962	29235261145554	191812548375979794
9	10077696	774840978	15251194969974	1185670253760822	23337547604774259426

Figure 5.1: *Numbers of feasible configurations, for a tiling of k rows, that each have l triangles in one row.*

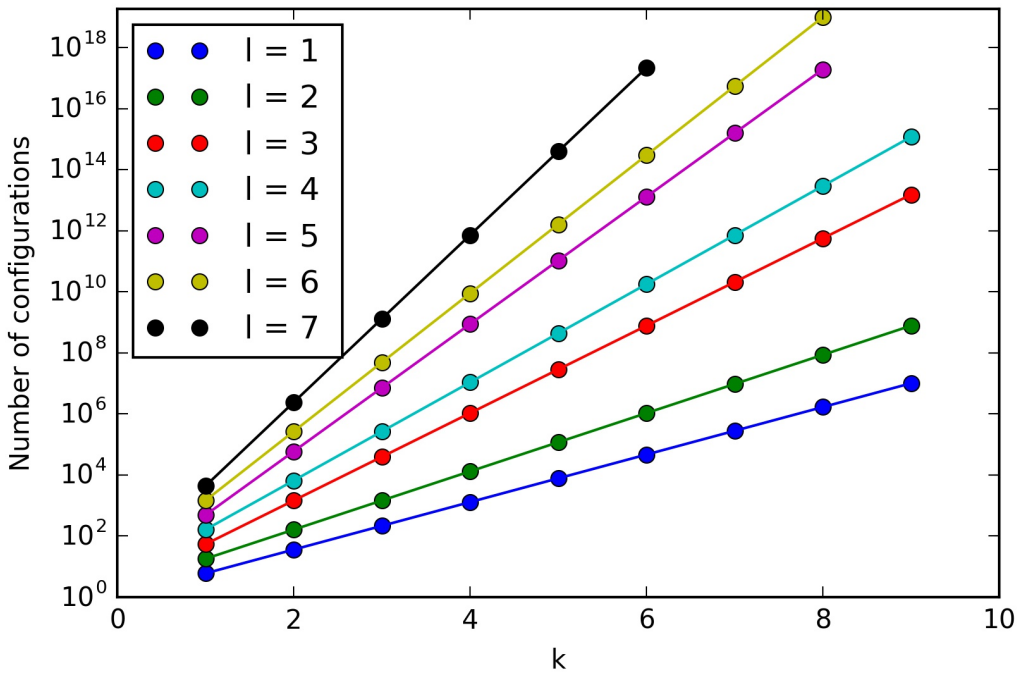

Figure 5.2: *Graph with the number of configurations plotted as function of k, for different values of l. Added are the exponential fits of these points, made in Python using* `curve_fit`.

points for a varying k and l fixed. This is done using curve_fit in Python. The values for a and b that resulted from these fits are given in Table 5.3.

We can see from Table 5.3 that a is approximately equal to $2^{\lfloor \frac{l}{2} \rfloor}$, and e^b is approximately equal to the limit of the ratio $\frac{a_{k,l}}{a_{k-1,l}}$. These ratios will be

l	a	b
1	1	1.79175947
2	2	2.19722458
3	2	3.29583687
4	3.99439862	3.70268795
5	3.99439862	4.80130024
6	7.97716814	5.20818619
7	7.97716814	6.30679848

Figure 5.3: *Values for a and b, for different values of l, using curve_fit in Python.*

given in Figure 5.4 in the next section.

5.2 Ratios between the different values

To find the ratios of the number of feasible configurations, we will fix one of the values k or l, and let the other increase. First of all, we will consider the ratio of the number of (k,l)-tilings and the number of $(k-1,l)$-tilings for different values of k and l. These ratios are given in Figure 5.4. Here, the case $k = 1$ is included, to give the starting value of the sequence. To get the number of feasible configurations for any (k,l)-tiling, we need to multiply the number of configurations for an $(1,l)$-tiling, with the ratio of the number of (i,l)-tilings and the number of $(i-1,l)$-tilings, for $i \in \{2,3,..,k\}$.

k/k-1 \ l	1	2	3	4	5	6
1	6	18	54	162	486	1458
2/1	6	9	27	40.55555555555556	121.66666666666667	182.7530864197531
3/2	6	9	27	40.556164383561644	121.66849315068494	182.76207525501587
4/3	6	9	27	40.55617104640951	121.66851313922854	182.76225786169798
5/4	6	9	27	40.556171119324794	121.66851335797439	182.7622614569721
6/5	6	9	27	40.55617112012275	121.66851336036825	182.7622615246456
7/6	6	9	27	40.55617112013148	121.66851336039444	182.7622615258783
8/7	6	9	27	40.55617112013158	121.66851336039474	182.7622615259003
9/8	6	9	27	40.55617112013158	121.66851336039474	182.76226152590067

Figure 5.4: *Ratios of the number of configurations for a row consisting of k triangles over the number of configurations for a row consisting of $k-1$ triangles.*

Example 5.2.1. If we for example want to find the number of feasible configurations, for a tiling of 4 rows, with 5 triangles in one row, we can find these by multiplying the element in row 1, column 5 in the table, so 486, by $121.66666666666667 \cdot 121.66849315068494 \cdot 121.66851313922854 \approx 1801059.00$, which gives that the number of configurations for a tiling of 4 rows of 5 triangles is approximately equal to: 875314674.000000123. Due to a rounding error when the numbers of k and l get bigger, this will in general give an estimate for the number of feasible configurations.

If we now fix the value of k and look at the ratios between $a_{(k,l)}$ and $a_{(k,l-1)}$ this results in the values given in Figure 5.5. Just like in the other table, for $l = 1$, the number is given by the number of feasible configurations for a $(k, 1)$-tiling. If we want to determine the number of feasible configurations for any k, we can now multiply the number of configurations for $l = 1$, and this k, by the ratios for this given k.

k \ l/(l-1)	1	2/1	3/2	4/3	5/4	6/5
1	6	3	3	3	3	3
2	36	4.5	9	4.506172839506172	9	4.506240487062405
3	216	6.75	27	6.768632830361225	27	6.768965750185773
4	1296	10.125	81	10.167030771054549	81	10.167885116478693
5	7776	15.1875	243	15.271697767641815	243	15.273513473899428
6	46656	22.78125	729	22.939318072565854	729	22.94284516856989
7	279936	34.171875	2187	34.456700338152054	2187	34.46319966469515
8	1679616	51.2578125	6561	51.75673463515519	6561	51.7683017255361
9	10077696	76.88671875	19683	77.74277727713314	19683	77.76286269471244

Figure 5.5: *Ratios of the number of configurations for a row consisting of l triangles over the number of configurations for a row consisting of $l - 1$ triangles.*

Example 5.2.1 (Continued)**.** We can use the table in Figure 5.5 to get the number of configurations for a $(4, 5)$-tiling. We can find this by multiplying the element in the table in row 4 and column 1, in the table, which is 1296, by $10.125 \cdot 81 \cdot 10.167030771054549 \cdot 81 \approx 675397.1250000000719$. This is approximately equal to 875314674.000000093. Rounding this off, gives the same value as the one found before in Example 5.2.1.

Some important observation that we can make, is that the rows converge quickly. For l fixed, they are almost identical after the ratio $\frac{k}{k-1} = \frac{5}{4}$. For k fixed, the behaviour of $\frac{l}{l-1}$ for the odd and even cases of l is different. For $\frac{l}{l-1}$, with l odd, there are k triangles added to one side, just like

we did for the case where $k = 2$ and l is odd on page 31. For $\frac{l}{l-1}$, with l even, the newly added triangles are placed between those older triangles. If we now multiply the fractions $\frac{l+1}{l}$ and $\frac{l}{l-1}$ for l odd, we see that this is the ratio of the number of configurations for a tiling where a full column is added, over the number of configurations without this column. This results in the same ratios as the ones found for $k = \frac{l}{2}$, so we know that for k fixed and l even, the values in the columns have to be almost identical after the ratio $\frac{l}{l-2} = \frac{10}{8}$.

For any matrix, we can define the spectral radius, which is given by $\rho(A) = \max\{\lambda : \lambda \text{ eigenvalue of } A\}$. About this spectral radius, a few useful theorems are known, among which Gelfand's Formula [24].

Theorem 5.2.2. *(Gelfand's Formula) For any given matrix norm $||\cdot||$ on the space $Mat(n, \mathbb{R})$ of $n \times n$-matrices, with $A \in Mat(n, \mathbb{R})$, the following equality holds:*

$$\rho(A) = \lim_{k\to\infty} ||A^k||^{\frac{1}{k}}.$$

This suggests that the limit of the ratios converges towards the largest eigenvalue of the matrix. We can use this to find the limits of the successive ratios of the configurations for increasing k, keeping l fixed. We can find these to be the following: $l = 1 : 6, l = 2 : 9, l = 3 : 27, l = 4 : 40.5562 \approx \frac{1}{2}(41 + \sqrt{1609}), l = 5 : 121.669 \approx \frac{3}{2}(41 + \sqrt{1609})$. When l is even, these values correspond to the largest eigenvalue of the matrix $A_{\frac{l}{2}}$. We have to divide by 2, because we have to keep in mind the fact that the unit tiling we are attaching consists of two triangles per row or column. For l odd, these values are equal to the largest eigenvalue of $\frac{l-1}{2}$, multiplied by 3.

This can be explained as follows: Every time we add a new row, this corresponds to first adding one row of $\frac{l-1}{2}$ triangles, which gives a factor that is equal to the largest eigenvalue of the matrix $A_{\frac{l-1}{2}}$. After this we add one triangle on the right side of this row. For this there are 3 possibilities, and thus we obtain the factor 3.

Using the fact that the ratios quickly converge to these largest eigenvalues, we can derive the following estimations of the values in the table, using the fact that the ratio between the elements in the first row is equal to 3:

$$a_{k,l} = 6 \cdot 3^{l-1} \cdot (\text{largest eigenvalue of } A_{\lfloor \frac{l}{2} \rfloor})^{k-1}, \qquad \text{for even } l \tag{5.1a}$$

and

$$a_{k,l} = 6 \cdot 3^{l-1} \cdot 3^{k-1} \cdot (\text{largest eigenvalue of } A_{\lfloor \frac{l}{2} \rfloor})^{k-1}, \qquad \text{for odd } l. \tag{5.1b}$$

On the other hand, we can consider the ratios of $\frac{l}{l-1}$ in Figure 5.5, when keeping k fixed. If we look at the ratio's $\frac{a_{k,l+2}}{a_{k,l}} = \frac{a_{k,l+2}}{a_{k,l+1}} \cdot \frac{a_{k,l+1}}{a_{k,l}}$, we see that this is equal to the largest eigenvalue of the matrix A_k. Observing that the ratio between the elements in the first column is equal to 6, we can find an estimation for the values in the table. This gives:

$$a_{k,l} = 6^k \qquad \text{for } l = 1, \tag{5.2a}$$

$$a_{k,l} = 6^k \cdot (\text{largest eigenvalue of } A_k)^{\frac{l-1}{2}} \qquad \text{for odd } l, l \neq 1 \tag{5.2b}$$

and

$$a_{k,l} = \frac{6^k}{3^k} \cdot (\text{largest eigenvalue of } A_k)^{\frac{l}{2}} \qquad \text{for even } l \tag{5.2c}$$

We can now use Equations 5.1 and 5.2 to find an estimate for the number of configurations.

We can also give an estimate for the growth factor of the largest eigenvalue. From the numbers in the columns of 5.4 we see that the growth factor of $l/l-1$ is approximately equal to 1.50 for l even and 3 for l odd. If we thus extend the tiling by one column of two triangles, or equivalently by one row of $2l$ triangles, the growth factor in the other direction has to grow by a factor of approximately 4.5. Thus the largest eigenvalue of the matrix A_k has to grow with a factor of approximately 4.5. We have not yet been able to derive an exact way to find the limiting value of the growth factor yet, but this might be nice to do.

It is also possible to calculate the ratio of the number of configurations for a $(k, 2k)$-tiling, over the number of feasible configurations for a $(k-1, 2(k-1))$-tiling. Of course, we can do this by using the above algorithm or the estimations in 5.1 and 5.2. The values that followed from this, are: $\frac{a_{(2,4)}}{a_{(1,2)}} = 365$ and $\frac{a_{(3,6)}}{a_{(2,4)}} = 7412.12876$, but from these two values it was impossible to derive a relation. To get this relation, more points need to be considered.

5.3 Fixed boundaries

The next problem we considered was to simulate the number of feasible configurations for the tiling with given boundary conditions. These num-

bers can be used to find the distribution of the number of feasible configurations, as a function of the number of boundary spins pointing into the tiling. We performed this simulation for various tilings, see Figure 5.9, but we will discuss the case of the $(3, 8)$-tiling in this thesis.

In any (k, l)-tiling there are $2k + l$ boundary spins, so for the $(3, 8)$-tiling we find $2 \cdot k + l = 14$ boundary spins. From this follows that there are 2^{14} different spin configurations on the boundary, for all of which we have determined the number of feasible configurations in Python. After this, we have added all numbers belonging to the configurations that have i spins pointing into the tiling, for $i \in \{0, 1...14\}$. For the $(3, 8)$-tiling, this gives the numbers in the table in Figure 5.6. In Figure 5.7 these numbers are plotted.

i	Number of configurations with i spins pointing in.
0, 14	50390
1, 13	1420098
2, 12	16466932
3, 11	104362850
4, 10	406876666
5, 9	1039163020
6, 8	1801630602
7	2160157930

Figure 5.6: *Numbers of configurations with i spins pointing into the tiling.*

Note that the number of configurations, that have either i spins pointing in, or i spins pointing out, is symmetric around where half of the boundary spins are pointing in. This can be proven, using the invariance principle, in which we use the outer boundary as the invariant subset.

Something that can be noted is, and which is also shown in Figure 5.9, is, that for any $(k, 2)$- or $(1, l)$-tilings, that have all spins pointing in, or all spins pointing out, there are no feasible configurations. This fact can be argued as follows: we will try to construct a $(k, 2)$-tiling, with all spins on the boundary pointing in or all spins pointing out. We, for example, can take the configuration shown in Figure 5.8a, with $k = 3$, and all spins pointing in. The first spin of this row has to point down, but then all successive inner spins have to point down. Continuing with placing the spins so that they are pointing down, will give a contradiction, because

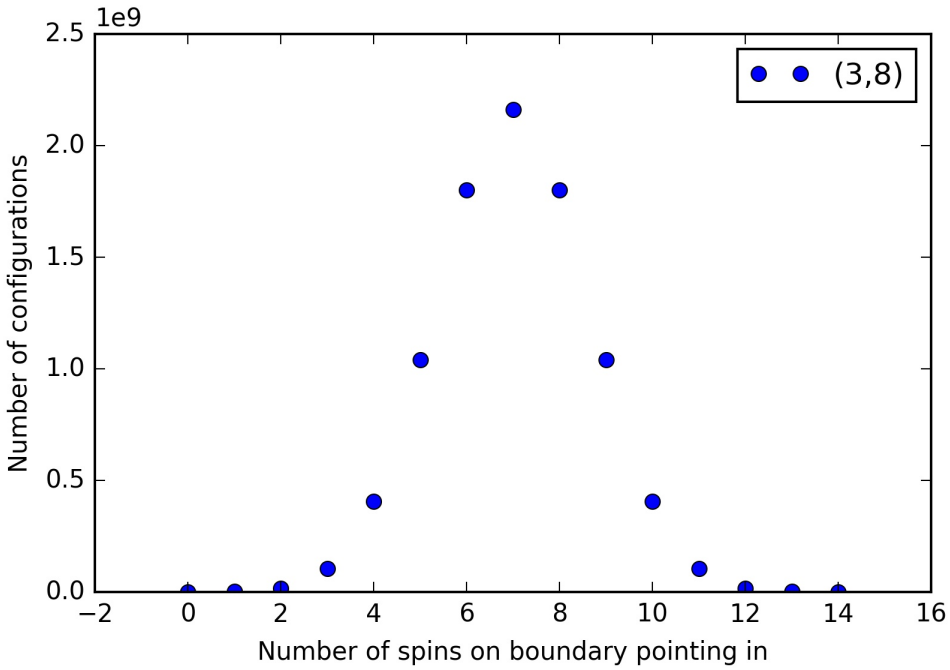

Figure 5.7: *The numbers of configurations for $(3,8)$-tiling, as a function of the number of spins on the boundary pointing into the tiling.*

the last spin can not be placed any more, as is visible in Figure 5.8b.

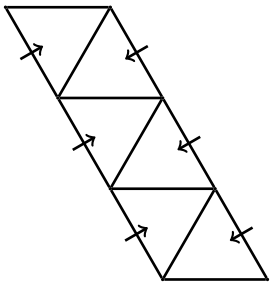

(a) *Boundary conditions for the $(3,2)$-tiling. For this configuration all spins are pointing in.*

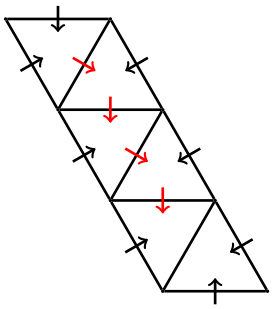

(b) *The (3,2)-tiling, where the outer spins are pointing in, and the inner spins can not be places, without frustration occurring.*

Figure 5.8

The lower boundary namely forces it to be pointing into the opposite direction. This thus yields frustration in the system, so there are no feasible configurations for the $(k,2)$- or $(1,l)$-tilings where all spins are pointing in

or all spins are pointing out.

Once the configurations consists of more rows or columns, respectively, we can find a hexagon inside the tiling, in which the spins can rotate, and this thus gives that there are one or more feasible configurations, when all of the outer spins are pointing outwards, or when they are all pointing inwards.

Figure 5.9 gives an overview of the different distributions for several of the tiling sizes. From the normalized version, shown in Figure 5.10, we can deduce that the number of configurations with i spins pointing in is normally distributed.

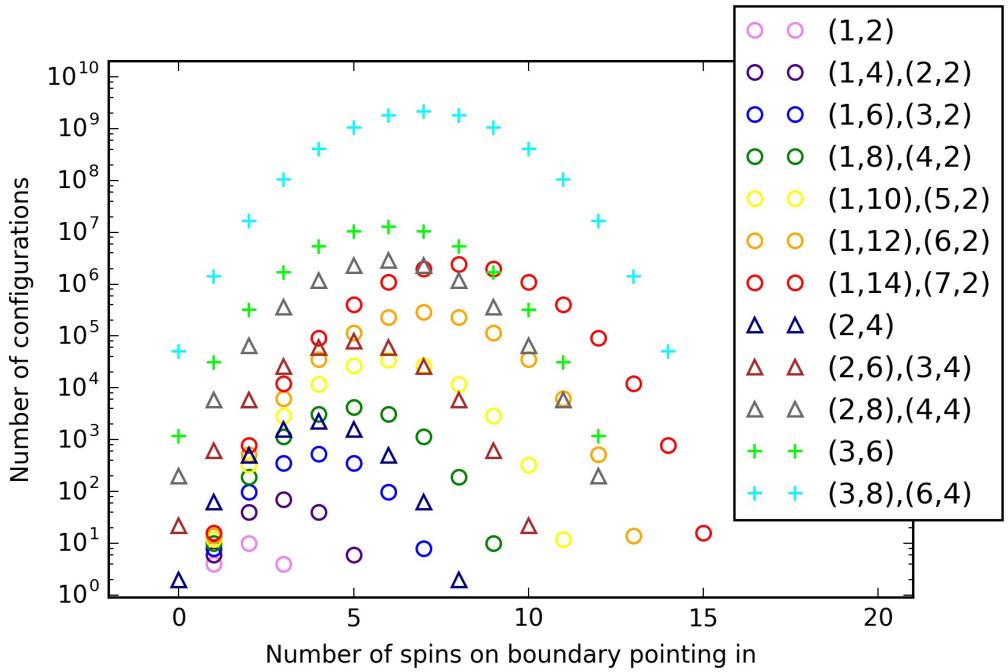

Figure 5.9: *The numbers of configurations as a function of the number of spins on the boundary (so all of the $2 \cdot k + l$ boundary elements) that are pointing into the tiling. For the configurations, where $k = 1$ or $l = 2$, the number of configurations, when all spins are pointing out, or all spins are pointing in, is equal to 0.*

These graphs can of course be normalized, which is shown in Figure 5.10. First the x-axis is rescaled, so that the number of spins pointing in is between 0 and 1. Scaling by the total number of configurations and $2k + l - 1$, the number of intervals between 0 and 1, then gives the normalized version of this graph, as shown in Figure 5.10.

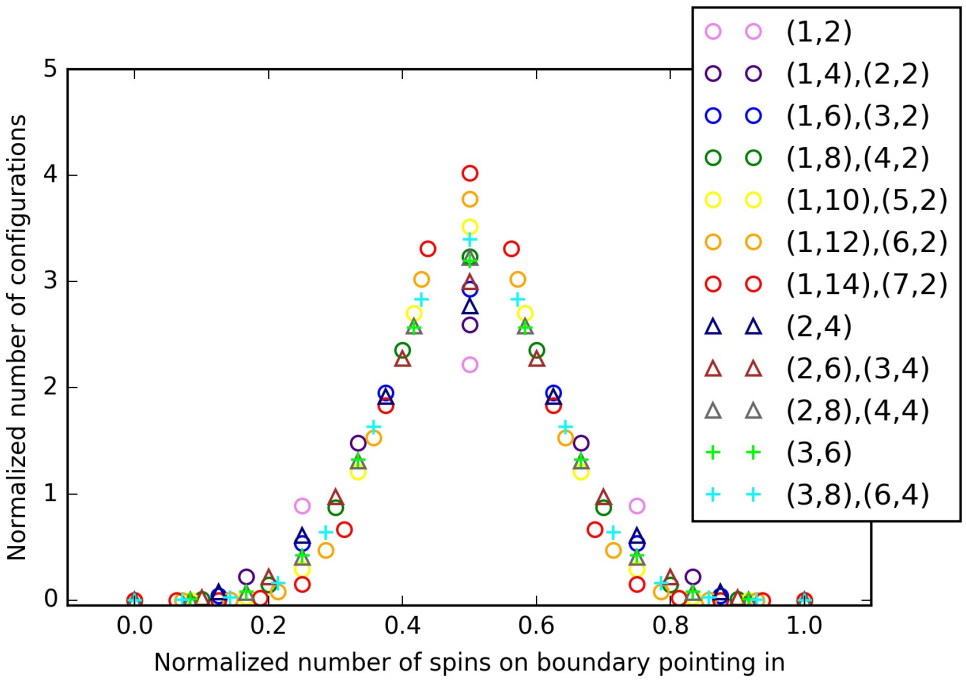

Figure 5.10: *The numbers configurations from Figure 5.9, but normalized.*

From Figure 5.10, we can see, that the maximum value for the number of configurations, can always be found, when half of the spins is pointing in and the other half is pointing out.

All these distributions are normalized and normally distributed. Since the number of data points is increasing, we can thus see from Figure 5.10, that the distribution of the number of elements is converging towards a continuous normal distribution. We know the mean of this distribution, which is equal to 0.5, because the maximum value for the number of configurations can always be found, when half of the spins is pointing in and the other half is pointing out. We have not derived the standard deviation of these distributions, but this is something that would be nice to do as well. From the figure we see, that if the size of the tiling increases, a bigger fraction of the configurations come close to 0.5, thus we expect that the standard deviation will decrease, as the tiling size increases.

In general, we thus know that if we have some (k,l)-tiling, that the probability to find a configuration where about half of the spins is pointing in is much bigger than the than the probability to find a tiling with very few or very much spins pointing in.

5.4 Number of reversible spins

5.4.1 Complex ordered patterns

Up to now, we have been looking at tilings, for which we have considered the way they were built up and have determined in how many ways this is possible. To this end, we have always considered finite tilings, of which we could deduce the exact properties. Kang, et al. [25] studied a triangular lattice, in which geometrical frustration is induced by buckling. In their article, they analyse the critical strain of buckled configurations of the triangular structures both analytically and with finite element simulations. The precise properties of these structures, like thickness and length of the beams can be found in [25].

The expected configurations the lattice will be buckling to, will be the ones with the smallest critical strain. They have been looking at a tiling, that has 11 rows of each 24 triangles. For this tiling, they found two eigenmodes that have a low critical strain. Looking at the center part of this tiling, so that the effects of the boundary are not too relevant any more, the two eigenmodes are periodically ordered patterns. These two are the so called symmetric pattern, as depicted in Figure 5.11a and the chiral pattern, depicted in Figure 5.11b.

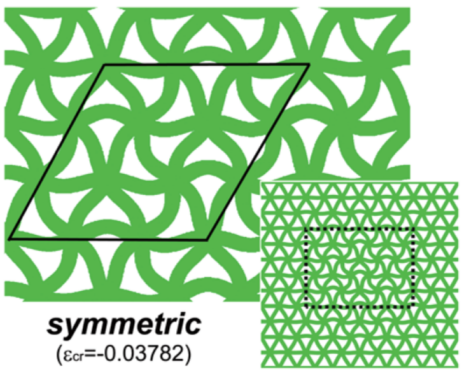

(a) *The symmetric configuration, with its critical strain and the center part of the tiling.*

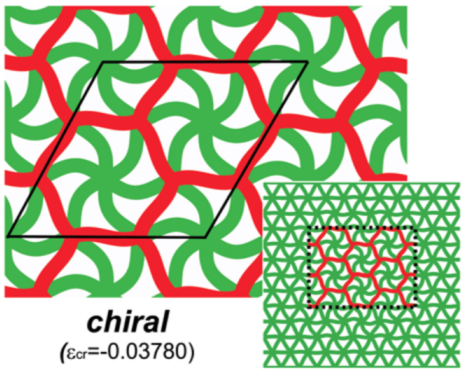

(b) *The chiral configuration, with its critical strain and the center part of the tiling. The beams that are coloured red, are the ones that buckle into a full sinusoid.*

Figure 5.11: *[25]*

To get rid of the boundary conditions, they also have considered infinite periodic triangular lattices, by using $(m, 2n)$-unit cells, having pe-

riodic boundary conditions. On this infinite periodic lattices, they have been looking at the critical strain of these tilings. For the $(3, 6)$-tiling, with the symmetric and chiral configurations, they found the lowest strain.

The symmetric and chiral patterns are similar to the tilings we have been considering before. The symmetric pattern has the exactly the same properties, while the chiral configuration has an interesting, different property. This different property is found in the beams that buckle into sinusoids. In Figure 5.11b, these beams are represented with a red color. In the chiral case, the sinusoidal beams are the only beams that can buckle to one of the sides–so that the spins on the edges point into one direction, like we have always been considering–without the occurrence of frustration in the system.

Something that can be investigated for any tiling, is the fraction of edges that can buckle into both directions. To this end, we will start by considering the symmetric and the chiral cases, where the sinusoidal edges are buckled into a predetermined direction. Because the pattern is periodic, in this counting we only have to consider the right or left boundary and the upper or lower boundary once. The other boundary is counted in the next unit cell.

5.4.2 Number of reversible spins for specific cases

For the symmetric case, counting gives that the fraction of spins of which the direction can be changed, without the occurrence of frustration is equal to $\frac{18}{27} = \frac{2}{3}$. In Figure 5.12, the different spins on the edges that can be reversed are shown in red. The spins on the edges that can not be reversed without causing frustration, are shown in green.

The dependence of the reversibility of these red spins is as follows. Two spins on adjacent sides (so sides that correspond to the same triangle) can not be reversed independently. For these cases, we really have to consider the configuration with one of the two spins reversed. For this configuration, we then have to look whether we can reverse the other spin as well. Two spins on edges of non-adjacent triangles can be reversed independently.

Let us now consider the chiral case. In order to change the direction of the green edges, we have to let the red sinusoidal edges be defined in one direction. Figure 5.13 shows a picture of a spin assignment so that nine of the green edges of the tiling (the light green edges) are not reversible. This

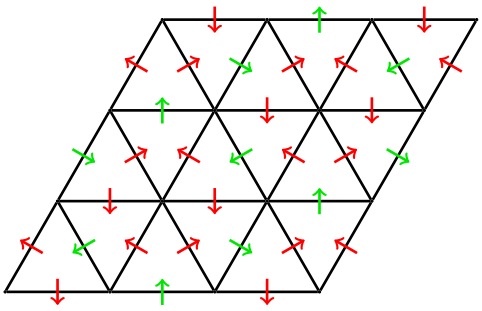

Figure 5.12: *The symmetric case. The red spins can be reversed, while the green spins have to remain pointing in the direction they were already pointing in. Reversing these green spins would cause frustration.*

is done by choosing the red edges in the way shown in the figure. All of the other spins (so the spins on both the red and the dark green edges) can be rotated.

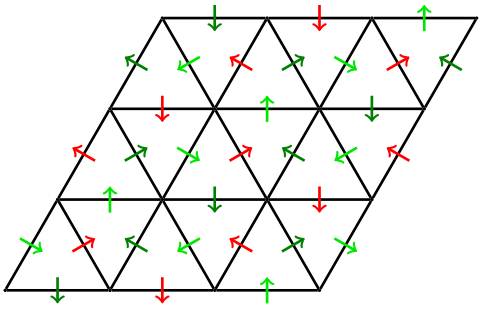

Figure 5.13: *Assignment of the spins to the red edges. The lighter green edges will be fixed by this assignment, while both the red edges and the dark green edges can still have their spins in both directions. In total, there are 18 edges, of which the spins can be reversed.*

We have constructed the tiling in Figure 5.13 in such a way, that maximizes the number of reversible spins. Since the direction of the red and dark green spins can both be changed, the fraction of elements that can independently be reversed is equal to $\frac{18}{27}$.

For this chiral case in Figure 5.13, the dependence of the reversibility of the spins is as follows.

The spins on non-adjacent edges can be reversed independently of each other, while the spins on two adjacent edges cannot. Since all of the red edges are non-adjacent, they can all be reversed independently. The same holds for the dark green edges. If we consider a pair of a red spin and a dark green spin that we want to reverse, then we need to know whether

the two edges are adjacent. If they are not, the spins can be reversed independently, but if they are adjacent, we again have to look at the configuration, where we have already reversed one of the two, and see whether it is possible to reverse the other one as well.

The above implies that the spins in one of the two inner hexagons, consisting of green spins that rotate around one point, can only all be fixed, if the spins around this hexagon point in the same direction (so either all in or all out). This is shown in Figure 5.14.

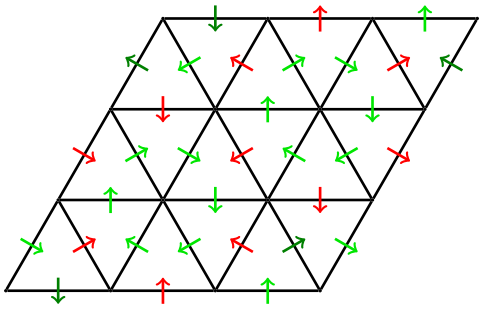

Figure 5.14: *Assignment of the spins to the red edges. The lighter green edges will be fixed by this assignment, while both the red edges and the dark green edges can still have their spins in both directions. Now there are twelve edges, of which the spin can be reversed.*

In the case in Figure 5.14, using the periodic boundary conditions, we have three dark green edges, and nine red edges that can be reversed. In total the fraction of spins that we are free to reverse, equals $\frac{12}{27}$. This assignment of the direction of the red spins is optimal for the chiral configuration. Indeed, reversing one (or more of these spins), will always result in just as many (or more) green spins that can be reversed, compared to the number that can not be reversed any more. Just like in the other chiral case, see Figure 5.13, we know that the red spins on the edges can be reversed independently of each other, just like all the green spins. Considering a pair of an adjacent red and green spin, we know that we again have to consider the configuration after we have reversed one of these spins to know whether we can also reverse the other spin.

We know with the symmetric case, and the first considered chiral case, that there are configurations that have eighteen of the twenty-seven spins that can be reversed. Thus, we would like to know, whether there are also configurations with periodic boundary conditions, that instead have eighteen of their twenty-seven spins fixed. This indeed is the case, see for example Figure 5.15.

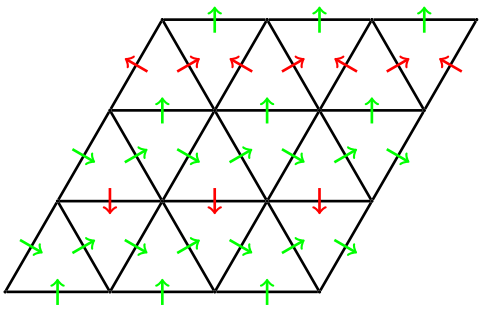

Figure 5.15: *Situation in which nine of the twenty-seven spins can be chosen. The red spins are the ones that can be chosen, the green ones are fixed.*

For this tiling there are nine, out of twenty-seven reversible spins. In this case, non-adjacent red spins can be reversed independently, while for adjacent red spins, we have to look at the configuration, after we have reversed one of the spins. Because of the symmetry of the system, we find that for all of these cases, the second spin will no longer be reversible. For the explanation of this, see Figure 5.16a.

5.4.3 Lower and upper bound on the number of reversible spins

We will first use the symmetric case, Figure 5.12, and the last case, Figure 5.15, to show why it is not possible to have less than 9 or more than 18 reversible spins, for a $(3,6)$-tiling. After this, we present a construction of a $(k,2n)$-tiling, that always has $\frac{2}{3}$ of the edges that can be reversed. Finally we will argue why $\frac{1}{3}$ is a lower bound for the number of reversible spins. Using this, it is possible to show that $\frac{1}{3}$ is a lower bound on the number of reversible spins, while $\frac{2}{3}$ is the maximum value.

For the symmetric case, we see that, for each one of the 18 triangles in the tiling, there are 2 sides, that are coloured red, so there are two sides that can be reversed. If we would only consider a single triangle that is not in a tiling, there are two sides that can be reversed. Hence, for each of the triangles in the $(3,6)$-tiling, the maximum amount of spins on edges that can be reversed is achieved, which is equal to 18. This implies that a fraction of $\frac{2}{3}$ of the whole system can be changed.

If we now consider the case in Figure 5.15, we will reverse the red reversible spins, and show that the number of reversible spins does not decrease. Because these red spins are the only ones that can be reversed, this

is the only option to change the tiling in Figure 5.15, by only changing one spin. Because of the periodicity of this tiling, we only have to consider two cases, namely one where we reverse one of the spins in the first row of triangles, and the case where we reverse one of the spins between the second and third row.

If we start with one of the spins in the first row, we get the configuration as in Figure 5.16a. For this case, there are four spins of which the reversibility is influenced. Of these four, there are two spins that were free to be reversed before, but can no longer, and two that could not be reversed, but can now.

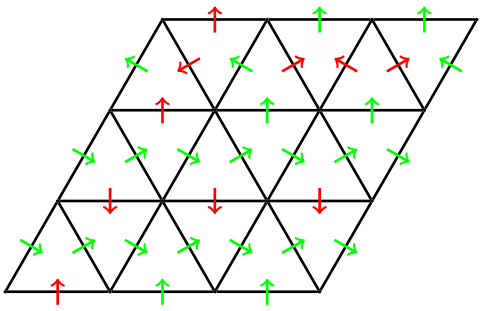

(a) *The case of Figure 5.15, where the second spin in the first row of triangles is reversed. Reversing this spin induces the tiling shown in this figure.*

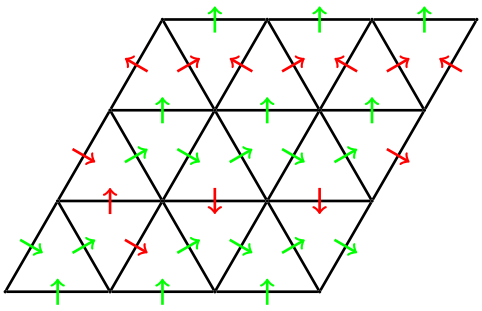

(b) *The case of Figure 5.15, where the first of the three spins between the second and third row of triangles is reversed. This results in this figure.*

Figure 5.16

For reversing the first spin between the second and third row, we will get the configuration as depicted in Figure 5.16b. In this case, we only get two spins that could not be reversed previously, but can now. The other two spins that are in the triangles, adjacent to this edge, could not be reversed and still can not. This implies that we gain two extra reversible spins. With the spin configuration in Figure 5.15, we thus can not create a tiling with less reversible spins, by only changing the direction of one of the reversible spins.

If we want to get less reversible spins, we need more spins to become fixed, compared to the amount of spins that become free to be reversed. To be able to reverse a spin, with the objective that more reversible spins become non-reversible, we need the spins to be oriented (apart from directional symmetries) as in Figure 5.17. We have tried to complete this tilling in several ways, but all of them gave at least 10 reversible spins.

For every extra spin (so for more than 9 spins), we could find another version of the pattern in Figure 5.17, for which we could reverse the center

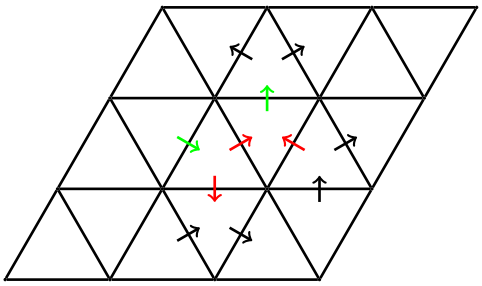

Figure 5.17: *The configuration needed to get less spins that can be reversed (apart from rotations or the interchanging of the spins). If we reverse the center spin, the number of reversed spins will decrease. The red spins are the ones that can be chosen, the green ones are fixed and for the black ones it is not yet determined, whether they will be fixed or not.*

spin and get less reversible spins. When we reversed this center spin, we obtained a pattern with less reversible spins. On the other hand, reversing any of the other reversible spins, would only result in patterns with an equal amount of reversible spins or more. Since these patterns only occur, when there are 10 or more reversible spins, this yields that nine is the minimum number of reversible spins.

For any other $(k, 2n)$-tiling, we can derive that the maximum fraction of reversible spins in a tiling is equal to $\frac{2}{3}$. This can be done, using the unit cell in Figure 5.18. Here the red spins can be reversed. Now we can construct a $(k, 2n)$-tiling, by attaching k of these unit tilings in one column, and attaching n rows of these columns next to each other. Then the fraction of reversible spins, is equal to $\frac{2}{3}$.

We can derive that the number of reversible spins for any other tiling cannot be larger than $\frac{2}{3}$. Suppose that a larger fraction than $\frac{2}{3}$ of the spins is reversible. Then, there has to be a triangle, that has 3 reversible spins. But this gives a contradiction. Thus, we find that $\frac{2}{3}$ is the maximum value for the number of reversible spins.

In the same way, we can apply the same reasoning to find the minimum value. For this we have to connect as many non-reversible sides to reversible sides. Since there is one non-reversible edge for each triangle and we have periodic boundary conditions, we find that there are configurations in which we can restrict $\frac{1}{3}$ of the reversible spins of the tiling to become non-reversible, by connecting them to non-reversible sides. Since $\frac{1}{3}$ of the spins already was not-reversible, we find that at most $\frac{2}{3}$ of the spins can be non-reversible. Hence, we have that at least a fraction of $\frac{1}{3}$ of

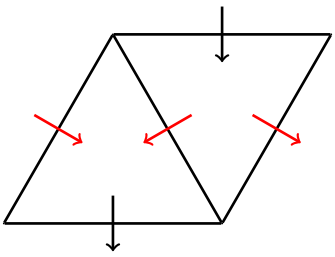

Figure 5.18: *The unit cell, that can be used to create a tiling with periodic boundary conditions. If the tiling is entirely built with this unit cell, the fraction of reversible spins is equal to* $\frac{2}{3}$.

the spins has to be reversible. The connection of the non-reversible sides to reversible sides is not always completely applicable, because in some cases the periodicity of the system limits the number of triangles that can be connected in this way. This is for example the case for an $(1,2)$-tiling:

Example 5.4.1. For all of the periodic $(1,2)$-tilings, we can determine the number of reversible spins. Note that if the spins on one of the two triangles are given, then the spins on the second triangle are also fixed.

Since each triangle has two sides that can be reversed, it follows that for the $(1,2)$-tilings, there also are 2 out of the 3 periodic boundaries that can be reversed. Thus we find in all of the cases of a periodic $(1,2)$-tiling, that the fraction of reversible spins is equal to $\frac{2}{3}$.

The above thus gives a reasoning, why $\frac{1}{3}$ forms a lower bound for the number of configurations, while the example gives a reasoning why it is not equal, but does not prove this. Hence we will state this as a conjecture.

Conjecture 5.4.2. Fix k and l. Consider the set of all (k,l)-tilings. The maximum lower bound on the fraction of independently reversible spins in these tilings is equal to $\frac{1}{3}$.

This can probably be proven by contradiction, using the reasoning given for the case that is illustrated in Figure 5.15.

Chapter 6

Discussion and Outlook

6.1 Discussion

In this thesis, we have been looking at tilings, in which the tiles satisfy the "two in-one out, or two out-one in"-relation. We have found the number of feasible configurations, for both the hexagon and any one-dimensional triangular (k, l)-tiling. For this last one, we also found an efficient way of determining this number. This is done, by an algorithm, in which we calculate the number of feasible configurations for all $(k, 2)$-tilings, where the spins on the left and right boundary are given. These $(k, 2)$-tilings can then be iteratively extended to a (k, l)-tiling.

It is of course also possible to extend this algorithm to compute the number of individual tilings with any predetermined boundary conditions. Besides this–instead of the problem with the voxels–we could also make a three-dimensional version of the problem addressed in this thesis, by placing more layers of a two-dimensional triangular lattice on top of each other. To do this, we need to define the locations of the edges between these layers. This last can for example be done in such a way that the unit cells become regular tetrahedrons or triangular prisms. Of course, we would then need to define some new constraints on the spins of the unit cells.

When the number of feasible configurations for all spins on the boundaries of the unit tilings are known, we can also apply this to derive the values for all of the symmetric $(k, 2k)$-tilings, by first extending the tiling by one row, and after this by one column. If we would know more about the number of feasible configurations of these tilings, we could derive the ratio with which these tilings are growing. With this, there might be a possibility to find a relation between the numbers of configurations of $(k, 2k)$-

tilings for different k.

We have also found a way to estimate the number of configurations, in an easier way. To do this, we made an approximation of the growth factor of the largest eigenvalue of the matrix A_k. The limit of this value, did not seem to converge exactly to 4.5, but to some value around 4.50639. It would be interesting to study this number and find the real value to which the largest eigenvalue is converging. Using this newly found value would allow for a better estimate of the number of feasible configurations of the tiling. Another thing that is useful to do, is to prove for each $k \in \mathbb{R}$, whether the Jordan Normal Form of the matrix A_k has a component in the direction of the eigenvector corresponding to the greatest eigenvalue.

A derivation of the distribution of the number of feasible configurations with i spins on the boundary pointing in, is given. Something that could still be done, is find some numerical algorithm, to derive these numbers of feasible configurations, which might give some new insights in the properties of the configurations of the tilings. We could also look at this limit distribution as the tiling size grows to infinity. For this limit distribution we can then derive the standard deviation, so that we can determine the numbers of configurations, when we would take k and l really large or infinite.

For the last problem addressed, we have looked at the number of independently reversible spins in a periodic $(k, 2n)$-tiling. For this, we showed that the maximum fraction of reversible spins is equal to $\frac{2}{3}$. We have stated a conjecture, that $\frac{1}{3}$ is a maximum lower bound on this same fraction. Something that still needs to be done, is to proof this conjecture. When this is done, it could be relevant to find the minimum fraction of reversible spins for every tiling size and look at the relation between these values. Another thing that can still be done, is deriving the limiting distribution of tiles for which i spins can be reversed. From this, it might also be possible to derive an estimate for the number of feasible configurations, by summing–or in the limit integrating–over all values.

Other things that we would be interested in, is to study the relation between the voxels and this problem. The voxel problem has more constraints than our problem. It would be nice to study the reason why this is true. Some important things that have not been considered very intensively yet, are holographic ordering and periodicity. It would be relevant

to consider why there are so few constraints, compared to the problem with the voxels.

It is also possible to consider the relation between our problem and the transfer matrix, that is used to solve the problems in the ice models in 2.2. We have not been looking at this, but it might be, that our methods for the derivation could be similar to the problems discussed in their models.

Something else, that would be nice to do, but is much more complicated, is to explore the invariance principle more thoroughly. It would be interesting to find a proof for the invariance principle on any tiling, where all of the possible combinations of spin configurations are used as an invariant subset.

6.2 Outlook

The main goal of this thesis, which was to find a way to calculate the number of feasible configurations for a (k, l)-tiling, proved to be solvable. We have found a way to derive this number and an estimate of the number of configurations. We derived the distribution of the number of feasible configurations, when i spins on the boundary are pointing into the tiling. Apart from this, we considered the number of spins in a periodic tiling that can be reversed, independently of the other spins. We showed that the maximum value for this is given by $\frac{2}{3}$, and stated a conjecture that the maximum lower bound is equal to $\frac{1}{3}$.

Appendix A

The Backtracking Algorithm

To calculate the number of configurations with Python, for a (k, l)-tiling, using the algorithm in Section 4.5, we need the matrix with the elements of the different configurations in the following way. Consider all 12 different triangles that can be formed, using the spins on the boundary, as depicted in Figure A.1. If two edges i and j can be connected, i.e. the spins on the edges are pointing in the same direction, then the matrix has a 1 as (i, j)-th and (j, i)-th element. The matrix found in this way is shown in Figure A.2.

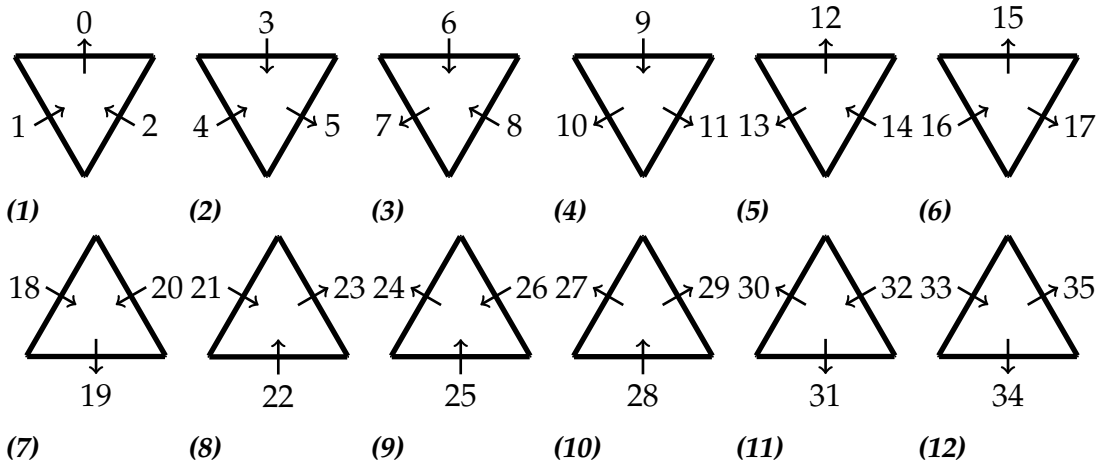

Figure A.1: *The twelve different configurations for the spins on the boundary. Every side of the twelve triangles has a unique number. These numbers are used to create a table, which gives all the edges that can be connected, by giving a 1 in the matrix, if two sides can be connected. As is normal to Python, we start with counting the edges from 0.*

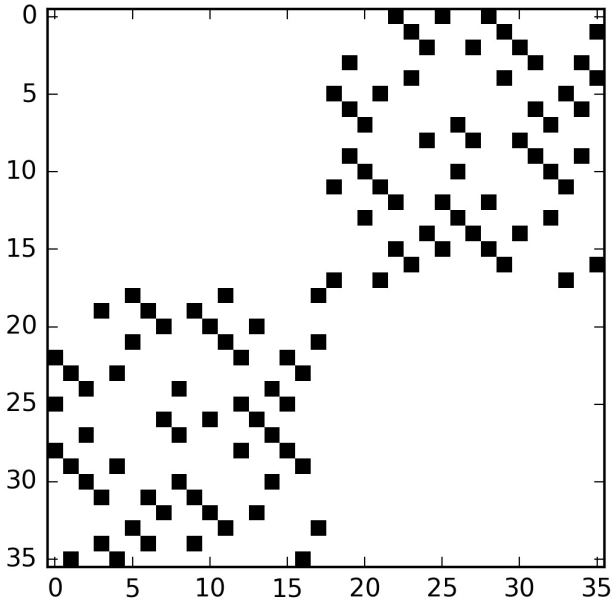

Figure A.2: *The matrix with the different combinations of the sides. If two sides i and j can be connected, the element i, j is black, so the value of the element of the matrix is 1, if they cannot, the element is white, hence the value of the element of the matrix is 0.*

With these, we can derive the number of configurations for a (k,l)-tiling, with the following algorithm. Here `ArrayPos.npy` is the matrix with the edges that can be placed next to each other, as shown in A.2.

Algorithm A.1: *Algorithm to calculate the number of configurations.*

```
# -*- coding: utf-8 -*-
"""
Calculates the number of configurations for a $(k,l)$-tiling, that looks as
follows:
 _______
\/\/\/\/\
 _______
 \/\/\/\/\
  _______
"""


import numpy as np

# Load matrix with possible configurations in CONF
CONF=np.load('ArrayPos.npy')

# Make TILES, of which the edges will get values from 0 to 35, to correspond
```

```
# with edges of the 12 possible triangles, of which the combinations with other
# sides that are possible are given by CONF.
TILES=[]

# Build TILE, consisting of the triangles. For triangles with the tip pointed
# upwards, we get TILE[1] = leftside, TILE[2]=lower side TILE[3]= rightside.
# For triangles with point upwards, we get TILE[1]= upper side TILE[2]=leftside
# TILE[3]=rightside. These tiles are added to TILES.

for i in range(0,6):
    TILE=np.zeros([3,1])
    TILE[0]= i*3
    TILE[1]= i*3 +1
    TILE[2]= i*3 +2
    TILES.append(TILE)

for i in range(6,12):
    TILE=np.zeros([3,1])
    TILE[0]= i*3
    TILE[1]= i*3 +1
    TILE[2]= i*3 +2
    TILES.append(TILE)

TILES.append(np.zeros([3,1])-1)

#############################################################################

# define all of the combinations of k and l, to be able to walk over all of the
# tiles in the whole tiling.
def walk(l,k):
    A=np.zeros([l*k,2])
    i=0
    for t in range(l):
        for v in range(k):
            A[i,0]=t
            A[i,1]=v
            i=i+1
    return A

#############################################################################

# For every triangle, the matrix B with an enumeration of the sides of these
# triangles is constructed. This enumeration is used to find all the triangles
# that can be attached on the next considered location.
def assigning_tiles(FIELD,tile,p,q,k,l):
    if(tile==-1):
        FIELD[ 3*int(p):3*int(p) + 3, int(q):int(q)+1 ]=np.zeros([3,1])-1
    else:
        FIELD[3*int(p):3*int(p)+3, int(q):int(q)+1 ]=TILES[int(tile)]
    return FIELD

#############################################################################

# This checks for every triangle, whether this triangle and the triangle on
# the side it wants to attach to exist, and whether the triangle is on the
# boundary, so that the neighbouring triangle is outside the tiling.
# If they both exist and the neighbouring element is not outside the tiling,
# this checks whether the triangles can indeed connect, as given by the
# configuration matrix.
def check_local(B,i,j,k,l):

    # triangles with tip pointing down
```

```
    if ((i%2== 0 and 0 == (i+j)%2 ) or (1==i%2 and 1==(i+j)%2 )):
        # left side;
        if (j>0 and not B[int(3*i+2),int(j-1)]==-1 and not B[int(3*i+1),int(j)]==-1):
            if( not CONF[int(B[int(3*i+2),int(j-1)]),int(B[int(3*i+1),int(j)])]):
                return False
        # right side;
        if (j<l-1 and not B[int(3*i+2),int(j)]==-1 and not B[int(3*i),int(j+1)]==-1):
            if( not CONF[int(B[int(3*i+2),int(j)]),int(B[int(3*i),int(j+1)])]):
                return False
        # upper side;
        if (l%2== 0):
            if (i>0 and not B[int(3*i),int(j)]==-1 and not B[int(3*i-2),int(j+1)]==-1):
                if( not CONF[int(B[int(3*i),int(j)]),int(B[int(3*i-2),int(j+1)])]):
                    return False
        elif (l%2== 1):
            if (i>0 and j<l-1 and not B[int(3*i),int(j)]==-1 and not B[int(3*i-2),int(j+1)]==-1):
                if( not CONF[int(B[int(3*i),int(j)]),int(B[int(3*i-2),int(j+1)])]):
                    return False

    # triangles with tip pointing up
    if ((0==i%2 and 1==(i+j)%2 ) or (1==i%2 and 0==(i+j)%2)):
        # left side;
        if (j>0 and not B[int(3*i+2),int(j-1)]==-1 and not B[int(3*i),int(j)]==-1):
            if( CONF[int(B[int(3*i+2),int(j-1)]),int(B[int(3*i),int(j)])]==0):
                return False
        # right side;
        if (j<l-1 and not B[int(3*i+2),int(j)]==-1 and not B[int(3*i+1),int(j+1)]==-1):
            if( CONF[int(B[int(3*i+2),int(j)]),int(B[int(3*i+1),int(j+1)])]==0):
                return False
        # lower side;
        if (i <k-1 and not B[int(3*i+1),int(j)]==-1 and not B[int(3*i+3),int(j-1)]==-1):
            if( CONF[int(B[int(3*i+1),int(j)]),int(B[int(3*i+3),int(j+1)])]==0):
                return False

    return True


##############################################################################

def solutions(k,l):
    solutions=0
    N=l*k
    A=np.zeros([k,l])-1
    n=0
    B=np.zeros([k*3,l])-1
    C=walk(k,l)

    while True:
        if n<0:
            break

        #To go over all possible combinations of k and l.
        i,j=C[n,0],C[n,1]
        A[int(i),int(j)]=A[int(i),int(j)]+1
        B=assigning_tiles(B,A[int(i),int(j)],i,j,k,l)

       # print n
       # print A
       # print B

        # If we have considered all of the 12 possible triangles, we will
        # return to the location of the tiling, that was considered before this.
```

```
        if(A[int(i),int(j)]>11):
            A[int(i),int(j)]=-1
            B=assigning_tiles(B,A[int(i),int(j)],i,j,k,l)
            n=n-1

        elif(check_local(B,i,j,k,l)):
            if(n==N-1):
                # A feasible configuration is found, so we add 1 to the number
                # of found configurations.
                solutions = solutions + 1
            else:
                # goes to the next tile
                n=n+1

    return solutions



################################################################################

# fill in (k,l), where k is the number of rows, l is the number of triangles in
# one row.

k=2
l=3

S= solutions(k,l)
print(k, l)
print(S)
```

Appendix B

Relevant definitions

All of these definitions have been mentioned in the thesis, but are stated here to serve as a quick back-up.

Definition B.0.1. *The* Poisson's Ratio *is the negative ratio of the strain in the transversal direction, the direction perpendicular to the direction in which a load is applied, over the strain in the axial direction, the direction in which a load is applied. If we assume the material is pulled on in the x-direction, then the Poisson's Ratio is equal to*

$$\nu = -\frac{\epsilon_y}{\epsilon_x},$$

where ϵ_y is the strain in the y-direction, so the change in length in the y-direction over the old length in the y-direction and ϵ_x is the strain in the x-direction.

Definition B.0.2. *A* plane tiling *is a countable family of closed sets $\mathcal{T} = \{T_1, T_2, ...\}$, of which the union $\bigcup T_i$ is the whole plane (in general $\mathbb{R}^2$), and for which the interiors are non-intersecting, i.e. for the interiors $T_i^\circ and T_j^\circ$ of T_i and T_j respectively, we have: $T_i^\circ \cap T_j^\circ = \emptyset$, for all $T_i, T_j \in \mathcal{T}$. [10]*

This means a plane tiling is thus a filling of some two-dimensional plane with non-overlapping two-dimensional shapes.

$T_1, T_2, ...$ are called the tiles *of $\mathcal{T}$.*

Definition B.0.3. *A tiling is called* frustrated *if there exist two tiles in this tiling, that have one edge in common, and the associated spins on this edge are not pointing in the same direction.*

Definition B.0.4. *The* spin pattern *or* spin configuration *is the way the spins on (a subset of) the edges of the tiles are placed.*

Definition B.0.5. *The* Bulk Modulus *of a material is the resistance of this material to uniform compression.*

The Shear modulus *of a material is the ratio of the shearing force divided by the area, over the shearing strain. Here, shearing is the phenomena of two unaligned forces acting on some material into the opposite direction.*

Definition B.0.6. Voxels *are 3-dimensional cubic unit cells, which can be contracted and extended along one of the axes, and then extend and shrink along the other axes, respectively. These voxels thus satisfy the "Two in-one out, or two out-one in" relation, as do the triangles we consider in this thesis. The different possible configurations are given in Figure 2.1.*

Definition B.0.7. Holographic ordering *is the phenomena for the big cube consisting of voxels, that the bulk is predefined by the surface of the cube. This comes from the fact, that if a spin is pointing out of a voxel on one side, then it also has to be pointing out of the voxel on the other side. Hence the directions of the spins have to be alternating. Thus, the surface of the cube is giving restrictions on the whole cube.*

Definition B.0.8. *The* Invariance principle *states that reversing all the spins on a particular subset of the edges, will not change the number of feasible configurations.*

We will call this particular subset of the edges the invariant subset*. Note that only the spins on this invariant subset are given, all of the other spins are not defined, they can still point in both directions.*

Definition B.0.9. *The* outer spins *are the spins that can be found on the edges on the boundary of the tiling.*

The inner spins *are the spins that can be found on the edges in the interior of the tiling.*

Definition B.0.10. *The* fraction of free spins *is the fraction of the spins, of which the direction can be reversed, without this causing frustration in the system, over the total amount of spins in the system.*

Acknowledgements

July, 8 2016

Today, we went on the lab excursion of the soft matter physics groups to finish the year. We have had a wonderful afternoon of milking and feeding cows, making cheese and eating pizza. I would like to thank all the people in Martin's, Daniela's, Luca's and Vincenzo's research groups for the great afternoon. It was a great way to finish the period of working on my bachelor's project. To the first three, also thanks for the great discussions during all of the lunch breaks about important, or sometimes less important subjects. I liked being part of your groups during my bachelor project, it was a great way to find out about all the different part of the university I did not know too much about before.

I would like to thank Peter Dieleman for the code on backtracking he has explained and given to me. Since about al my knowledge on Python has been declining over the last three years, it was very useful to have something to build further on and to remember the basics of Python again. Your code has proven to be very useful for about all of the Python programmes I have been writing.

I would also like to thank Chris, Joseph, Niek and Quinten. We have had an amazing time together in the room, making traps for each other at the door, me trying to convince you to play soccer in the hallway instead of in the room, throwing things at each others heads and trying recognising all cities, visible out of the window. But apart from this, also thanks for the relevant discussions that we have had on our theses and projects. I really feel like I have been learning a lot from your projects as well.

My parents, for their support and all the trust they had in me, that I would make the right decisions on the things I wanted to do. Thank you for everything. My little sisters, for distracting me at the times I really needed this. You are amazing!

Last but not least, I would like to thank my supervisors. It was great to work with you. First of all, Floske, for all your support in the writing of my thesis, checking it over and over again for mistakes, and making sure there was enough mathematics in it. Martin, for all your support in the process of finding what I was really looking for, and making sure I explored more applications, instead of getting stuck into details too much. Despite the fact that you both have had an incredibly busy time, you both were everything I could have asked for during my project.

Rivka

References

[1] J. Christensen, M. Kadic, O. Kraft, and M. Wegener, *Vibrant Times for Mechanical Metamaterials*, MRS Communications **5**, 453 (2015).

[2] T. A. Schaedler, A. J. Jacobsen, A. Torrents, A. E. Sorensen, J. Lian, J. R. Greer, L. Valdevit, and W. B. Carter, *Ultralight Metallic Microlattices*, Science **334**, 962 (2011).

[3] J. L. Silverberg, A. A. Evans, L. McLeod, R. C. Hayward, T. Hull, C. D. Santangelo, and I. Cohen, *Using Origami Design Principles to Fold Reprogrammable Mechanical Metamaterials*, Science **345**, 647 (2014).

[4] R. S. Lakes, *Foam Structures with a Negative Poisson's Ratio*, Science **235**, 1038 (1987).

[5] G. W. Milton and A. V. Cherkaev, *Which Elasticity Tensors are Realizable?*, Journal of Engineering Materials and Technology **117**, 483 (1995).

[6] M. Kadic, T. Bückmann, N. Stenger, M. Thiel, and M. Wegener, *On the Practicability of Pentamode Mechanical Metamaterials*, Applied Physics Letters **100**, 191901 (2012).

[7] T. Bückmann, M. Thiel, M. Kadic, R. Schittny, and M. Wegener, *An Elasto-Mechanical Unfeelability Cloak made of Pentamode Metamaterials*, Nature Communications **5**, 3140 (2014).

[8] R. S. Lakes, *Negative Poisson's Ratio Materials*, `http://silver.neep.wisc.edu/~lakes/Poisson.html`, Accessed: March 03, 2016.

[9] C. Kettenis, *Designing the Response of Triangular Soft Mechanisms*, 2014, Bachelor's thesis at Leiden University.

[10] B. Grünbaum and G. C. Shephard, *Tilings and patterns.*, WH Freeman and Company, Co-published by Akademie-Verlag, 1987.

[11] C. Coulais, E. Teomy, K. de Reus, Y. Shokef, and M. van Hecke, *Combinatorial Design of Textured Mechanical Metamaterials*, (Unpublished).

[12] L. C. M. Kallenberg, *Besliskunde 4*, 2016, Syllabus (in Dutch).

[13] L. Pauling, *The Structure and Entropy of Ice and of Other Crystals with Some Randomness of Atomic Arrangement*, Journal of the American Chemical Society **57**, 2680 (1935).

[14] J. Snyder, J. S. Slusky, R. J. Cava, and P. Schiffer, *How 'spin ice' freezes*, Nature **413**, 48 (2001).

[15] E. H. Lieb, *Residual Entropy of Square Ice*, Physical Review **162**, 162 (1967).

[16] E. H. Lieb, *Exact Solution of the Problem of the Entropy of Two-Dimensional Ice*, Physical Review Letters **18**, 692 (1967).

[17] F. Rys, *Über ein Zweidimensionales Klassisches Konfigurationsmodell*, Helvetica Physica Acta **36**, 537 (1963).

[18] J. C. Slater, *Theory of the Transition in KH_2PO_4*, The Journal of Chemical Physics **9**, 16 (1941).

[19] E. H. Lieb, *Exact Solution of the F Model of an Antiferroelectric*, Physical Review Letters. **18**, 1046 (1967).

[20] E. H. Lieb, *Exact Solution of the Two-Dimensional Slater KDP Model of a Ferroelectric*, Physical Review Letters **19**, 108 (1967).

[21] F. Y. Wu, *Exact Solution of a Model of an Antiferroelectric Transition*, Physical Review **183**, 604 (1969).

[22] R. J. Baxter, *Eight-Vertex Model in Lattice Statistics*, Physical Review Letters **26**, 832 (1971).

[23] R. J. Baxter, *F Model on a Triangular Lattice*, Journal of Mathematical Physics **10**, 1211 (1969).

[24] P. Lax, *Functional Analysis*, Pure and applied mathematics, Wiley, 2002.

[25] S. H. Kang, S. Shan, A. Košmrlj, W. L. Noorduin, S. Shian, J. C. Weaver, D. R. Clarke, and K. Bertoldi, *Complex Ordered Patterns in Mechanical Instability Induced Geometrically Frustrated Triangular Cellular Structures*, Physical Review Letters **112**, 098701 (2014).